Stochastic-analytic approach to the calculation of multiply scattered lidar returns

Daniel T. Gillespie

Research Department, Naval Weapons Center, China Lake, California 93555

Received October 22, 1984; accepted March 18, 1985

For a laser that fires a short pulse at time 0 into a homogeneous cloud with specified scattering and absorption parameters, this paper addresses the problem of theoretically calculating $J_n(t)$, the nth-order backscattered power measured at any time $t > 0$. The backscattered power is assumed to be measured by a small receiver, which is colocated with the laser and which is fitted with a forward-looking conical baffle of adjustable opening angle. The approach taken here to calculate $J_n(t)$ is somewhat unusual in that it is not based on the radiation-transfer equation but rather on the premise that the laser pulse consists of propagating photons, which are scattered and absorbed in a probabilistic manner by the cloud particles. Polarization effects have not been considered. By using straightforward physical arguments together with rigorous analytical techniques from the theory of random variables, an exact formula is derived for $J_n(t)$. For $n \geq 2$ this formula is a well-behaved $(3n - 4)$-dimensional integral. The computational feasibility of this integral formula is demonstrated by using it to evaluate $J_n(t)/J_1(t)$ for a model cloud of isotropically scattering particles; for that case an analytical formula is obtained for $n = 2$, and a Monte Carlo integration program is employed to obtain numerical results for $n = 3, \ldots, 6$.

1. INTRODUCTION

In this paper we consider the following general problem: A pulse-type laser is situated on the ground and aimed vertically upward (see Fig. 1). The location of the laser defines the origin O of an xyz Cartesian frame, with the xy plane coinciding with the ground and the z axis pointing up. A cloud, composed of small particles with known radiation scattering and absorption properties, occupies the region $z \geq b$, where b is a given nonnegative constant. (We shall see later that the situation in which the ground is not physically present and the cloud fills all of space can be treated as a special case.) A receiver, which is capable of measuring backscattered laser radiation, is colocated with the laser. The receiver consists of a radiation-sensitive disk of radius r_0, lying in the xy plane and centered on the origin, together with an upward-pointing conical baffle, whose admittance angle is $2\psi_0 (0 < \psi_0 < \pi/2)$. The idea is that the receiver detects backscattered laser radiation from the cloud if and only if that radiation strikes the disk at an angle less than ψ_0 with the vertical. Assuming now that the laser fires a pulse at time 0, we want to calculate the quantity

$$J_n(t) \equiv \text{the power, measured by the receiver at time } t, \text{ that has been scattered exactly } n \text{ times by the cloud particles } (t > 0; n = 1, 2, \ldots). \quad (1)$$

The importance of this problem stems from the widespread use of pulsed lasers with colocated, forward-looking receivers (so-called monostatic lidar systems) to probe clouds. The purpose of the probing could be either to locate some object within the cloud or to investigate various physical properties of the particles that constitute the cloud. In such applications, interest is usually focused on the easily calculated quantity $J_1(t)$. But clearly, an exclusive interest in $J_1(t)$ can be justified only in those cases in which it can be confidently established that $J_n(t)/J_1(t) \ll 1$ for all $n \geq 2$.

The calculation of $J_n(t)$ presented here will be subject to several restrictive assumptions. All these assumptions seem reasonable for common lidar applications, but it is appropriate to state them clearly at the outset. First, although the cloud may contain any number of different types of scattering–absorbing particles, we require that these particles have a uniform random distribution inside the cloud, i.e., we require the cloud to be well mixed. Second, we require that the receiver disk be small; more specifically, we require that $r_0 \ll ct$, a condition that evidently imposes a positive lower limit on the observation time t. Third, we require that both the cross-sectional area and the angular divergence of the laser beam be entirely negligible, so that every photon in the initial laser pulse can be regarded as traveling along the $+z$ axis. And finally, we shall assume that the duration Δ of the laser pulse is essentially zero; however, this short-pulse assumption is not so crucial as the others, and we shall indicate how it can be relaxed if one wishes to use a specific pulse-shape function with a finite time duration.

The problem of computing $J_n(t)$ for $n \geq 2$ is not an easy one. It has been considered, in various guises, by several investigators using a variety of methods. Most approaches are *analytic* ones based on the radiation-transfer equation[1]; prominent among these are the treatments by Liou and Schotland,[2] Eloranta,[3] Weinman,[4] Carter *et al.*,[5] and Cai and Liou.[6] Other approaches have consisted of *Monte Carlo simulations*, among which are the works of Plass and Kattawar,[7] Blättner *et al.*,[8] and Kunkel and Weinman.[9] In spite of these many contributions, there seems to be no broad consensus that the problem of calculating multiply scattered lidar returns has been put to rest.

The approach taken in the present paper has several unique aspects. Although it is not feasible to make detailed comparisons here with all the works just cited, the following points should help to place our effort in context: (1) Even though our approach is *analytic*, in the sense that we derive an ex-

0740-3232/85/081307-18$02.00

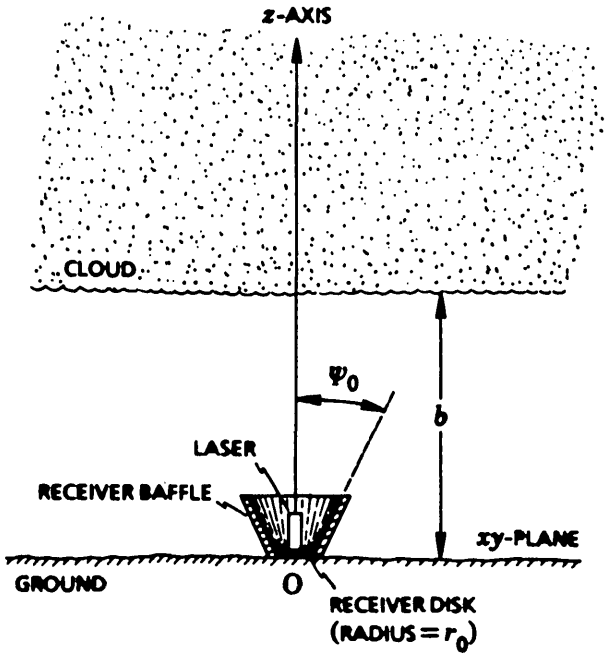

Fig. 1. The lidar configuration considered in this paper. The situation in which the ground is not present and the cloud fills all xyz space can be treated as a special case of this configuration.

plicit, closed-form expression for $J_n(t)$, we do not use or rely on the radiation-transfer equation. Instead, we proceed from the premise that the problem concerns a collection of propagating photons that are *stochastically* scattered and absorbed by the cloud particles. This is essentially the same premise that underlies most Monte Carlo simulations of the multiple-scattering problem (e.g., Kunkel and Weinman[9]), and it seems, at least to this writer, to afford a more easily visualizable picture of the relevant physical processes than does the radiation-transfer equation. (2) Probably the most novel feature of our treatment is its use of a somewhat esoteric theorem in random-variable theory called the random-variable transformation (RVT) theorem.[10] Application of this theorem is what allows us to pursue the stochastically formulated multiple-scattering problem in an analytic mode rather than in a simulation mode. (3) Our final expression for $J_n(t)$ for $n \geq 2$ is in the form of an explicit $(3n-4)$-dimensional definite integral. By comparison, the recent work of Cai and Liou[6] gives integral forms that are $(3n)$-dimensional. Like Cai and Liou, we shall normally evaluate these integrals for specific parameter values by using Monte Carlo techniques. In that connection, it is important not to confuse the Monte Carlo evaluation of a definite integral with the Monte Carlo simulation of a stochastic process. (4) Our analysis ignores the important but complicating fact of radiation polarization. In this respect, our analysis is not so ambitious as some previous ones (e.g., Cai and Liou[6]). We hope to investigate ways of incorporating polarization effects into our approach in a subsequent publication.

The plan of our work here is as follows: In Section 2 we show that the propagation of a photon through a cloud is an intrinsically stochastic phenomenon, and we derive expressions for the fundamental propagation probabilities in terms of the physical parameters of the cloud. In Section 3 we show how the calculation of $J_n(t)$ can be reduced, in most cases of physical interest, to the calculation of a certain probability function P_n. For $n = 1$ the function P_n can be calculated from the fundamental propagation probabilities easily and directly; we perform that calculation in Section 4 and thus arrive at a formula for $J_1(t)$. Section 5 describes the much more difficult and circuitous calculation of P_n for arbitrary n. For this, we first introduce an auxiliary probability function Q_n, and we then use the previously mentioned RVT theorem to write P_n as a multidimensional integral over Q_n times three Dirac delta functions. To render the integral suitable for numerical evaluation, we must analytically integrate out the delta functions and transform to a set of integration variables for which the integrand and the integration domain are both bounded. This (purely mathematical) phase of our derivation is unfortunately too lengthy to detail here, so we merely sketch a few of the highlights and then state the result; a complete account of the analysis can be found in a companion technical publication.[11] Our final computer-ready integral formula for $J_n(t)/J_1(t)$ is presented in Section 6 [in Eq. (50) for $n = 2$ and Eq. (51) for $n \geq 3$]. In Section 7 we demonstrate the computational feasibility of this formula by obtaining numerical results for $n = 2$ through 6 for a simple model cloud of isotropically scattering particles. Applications to more-realistic cloud models will be presented in a later publication.

In our work here, we shall make frequent use of two special mathematical functions. One, as just indicated, is the Dirac delta function δ, which is defined by the pair of equations

$$\delta(x - x_0) = 0 \qquad \text{if } x \neq x_0, \tag{2a}$$

$$\int_{-\infty}^{\infty} f(x)\delta(x - x_0)dx \equiv f(x_0) \tag{2b}$$

for any function f of x. The other special function that we shall use is the inequality function I, defined by

$$I(\text{inequality}) \equiv \begin{cases} 1 & \text{if inequality is satisfied} \\ 0 & \text{if inequality is not satisfied} \end{cases}. \tag{3}$$

For example, $I(a < x < b)$ is unity if x lies between a and b and is zero if x does not lie between a and b. The I function can generally be written in terms of the more familiar Heaviside step function, but for our work here the I-function notation proves to be less cumbersome.

2. STOCHASTIC SCATTERING AND ABSORPTION OF PHOTONS IN CLOUDS

It is not in general possible to predict with certainty the trajectory of a photon traveling through a cloud of randomly located scatterers and absorbers.[12] The best that we can hope to do is to assign probabilities to all possible trajectories; these in turn may be used to calculate various physically relevant averages. In this section we want to show that for almost any well-mixed cloud there exist two scalar constants β and β_s and a scalar function f such that the following two probability statements are true:

$$\exp(-\beta u) = \text{probability that a photon will move a distance } u \text{ in the cloud without being either scattered or absorbed,} \tag{4}$$

$\beta_s du \times f(\theta)\sin\theta d\theta d\phi$ = probability that a photon will be scattered, in the next infinitesimal distance du, into the solid angle $\sin\theta d\theta d\phi$ in the polar direction (θ, ϕ) relative to its present direction of travel.

$$(0 \le \theta \le \pi; 0 \le \phi < 2\pi). \quad (5)$$

Equations (4) and (5) are, for our purposes, the fundamental laws governing the propagation of a photon in a well-mixed cloud; they will form the physical basis for our analysis of lidar backscattering.

To derive Eqs. (4) and (5), and to see how the quantities β, β_s, and f are related to the physical parameters of the cloud, we suppose that the cloud consists of a randomly uniform mixture of various types of small particles. Let particle type k populate the cloud with an average density of ρ_k particles per unit volume. Further, let each type-k particle have, relative to the laser photons, a scattering cross section $\sigma_{s,k}$, an absorption cross section $\sigma_{a,k}$, and an angular scattering function $f_k(\theta)$. The physical significance of $\sigma_{s,k}$ is as follows: As a given photon moves an infinitesimal distance du in the cloud, it sweeps out relative to any type-k particle an infinitesimal scattering cylinder of length du and base area $\sigma_{s,k}$, in the sense that any type-k particle whose center happens to lie inside that cylinder will scatter the photon as it attempts to travel the distance du. Since the type-k particles are distributed uniformly at random throughout the cloud, then the probability that any particular type-k particle will have its center inside the scattering cylinder is just the ratio of the scattering-cylinder volume $\sigma_{s,k}du$ to the cloud volume V_c. Thus $\sigma_{s,k}du/V_c$ is the probability that any *particular* type-k particle will scatter the photon in the next du of its journey through the cloud. Since du is infinitesimal, the probability for more than one scattering in du is negligibly small compared with the probability for a single scattering; therefore the probability that *any* of the $\rho_k V_c$ type-k particles in V_c will scatter the photon is given by the product

$$(\rho_k V_c) \times (\sigma_{s,k}du/V_c) = \rho_k \sigma_{s,k} du.$$

We thus see that, if a photon is about to move an infinitesimal distance du in the cloud, then

$\rho_k \sigma_{s,k} du$ = probability that the photon will be scattered in du by a type-k particle. (6a)

And of course a similar argument shows that

$\rho_k \sigma_{a,k} du$ = probability that the photon will be absorbed in du by a type-k particle. (6b)

If we now define

$$\beta_s \equiv \sum_k \rho_k \sigma_{s,k}, \quad (7a)$$

$$\beta_a \equiv \sum_k \rho_k \sigma_{a,k}, \quad (7b)$$

$$\beta \equiv \beta_s + \beta_a \equiv \sum_k \rho_k (\sigma_{s,k} + \sigma_{a,k}), \quad (7c)$$

then it follows from Eqs. (6) and the addition law of probability theory that

$\beta_s du$ = probability that the photon will be scattered in the next du, (8a)

$\beta_a du$ = probability that the photon will be absorbed in the next du, (8b)

βdu = probability that the photon will be either scattered or absorbed in the next du. (8c)

Equation (4) can now be easily derived from Eq. (8c) by applying a well-known probability argument.[13] Using Eqs. (4) and (8c) together, it is easy to show that the mean free path of the photon in the cloud is β^{-1}. The constant β is identical to the so-called extinction coefficient of the cloud.

We assume that if a photon is absorbed by a cloud particle, then the photon is effectively eliminated from further consideration. However, if a photon is scattered by a type-k particle, it immediately changes direction in a manner determined by the angular scattering function f_k according to the following rule:

$f_k(\theta)\sin\theta d\theta d\phi \equiv$ probability that a photon, which has just been scattered by a type-k particle, will have its new direction of travel pointing in the infinitesimal solid angle $\sin\theta d\theta d\phi$, at polar angle θ and azimuthal angle ϕ relative to its previous direction of travel.

$$(0 \le \theta \le \pi; 0 \le \phi < 2\pi). \quad (9)$$

We are assuming that we are dealing with unpolarized photons and randomly oriented scatterers, so that f_k is independent of the azimuthal scattering angle ϕ. The function f_k clearly must be nonnegative; furthermore, since a scattered photon must emerge in some direction, the integral of f_k over the total solid angle must be unity; therefore f_k satisfies the normalization condition

$$\int_0^\pi f_k(\theta)\sin\theta d\theta = (2\pi)^{-1}. \quad (10)$$

Two commonly used simple models for light scattering are the isotropic-scattering model, for which $f_k(\theta) = (1/4\pi)$, and the Rayleigh-scattering model, for which $f_k(\theta) = (3/16\pi)(1 + \cos^2\theta)$. For a spherical dielectric particle (e.g., a water droplet), $f_k(\theta)$ would be the corresponding Mie-scattering function, normalized according to Eq. (10).

From Eqs. (6a) and (9), together with the multiplication law of probability theory, it follows that

$\rho_k \sigma_{s,k} du f_k(\theta)\sin\theta d\theta d\phi$ = probability that a photon will be scattered in the next du by a type-k particle into the solid angle $\sin\theta d\theta d\phi$ in the polar direction (θ, ϕ) relative to its present direction of travel $(0 \le \theta \le \pi; 0 \le \phi < 2\pi)$. (11)

Summing this probability over all k we obtain, through the addition law of probability theory, the probability that the photon will be scattered in the next du into the solid angle $\sin\theta d\theta d\phi$ at (θ, ϕ) by any type of particle. But this sum over k can be written as

$$\sum_k \{\rho_k \sigma_{s,k} du \times f_k(\theta)\sin\theta d\theta d\phi\} \equiv \beta_s du \left\{\sum_k (\rho_s \sigma_{s,k}/\beta_s) f_k(\theta)\right\} \sin\theta d\theta d\phi.$$

Therefore, by simply defining the function f to be

$$f(\theta) \equiv \sum_k (\rho_k \sigma_{s,k}/\beta_s) f_k(\theta), \tag{12}$$

we obtain at once the result in Eq. (5).

It follows from Eq. (8a) and the factored structure of the left-hand side of Eq. (5) that $f(\theta)\sin\theta \mathrm{d}\theta\mathrm{d}\phi$ may be interpreted as the probability that a photon, having just been scattered by an unspecified type of particle, will emerge in the solid angle $\sin\theta\mathrm{d}\theta\mathrm{d}\phi$ in the polar direction (θ, ϕ) relative to its previous direction of travel. By integrating Eq. (12) over θ and making use of Eqs. (10) and (7a), we can easily show that the function f satisfies the same normalization condition as the functions f_k:

$$\int_0^\pi f(\theta)\sin\theta \mathrm{d}\theta = (2\pi)^{-1}, \tag{13}$$

The twofold purpose of the foregoing analysis was to provide a physical rationale for the probability statements in Eqs. (4) and (5) and also to indicate how the parameters β_s, β, and $f(\theta)$ contained in those equations are related to more-conventional cloud parameters. We found that

$$\beta_s = \sum_k \rho_k \sigma_{s,k}, \tag{14a}$$

$$\beta = \sum_k \rho_k (\sigma_{s,k} + \sigma_{a,k}), \tag{14b}$$

$$f(\theta) = \beta_s^{-1} \sum_k \rho_k \sigma_{s,k} f_k(\theta). \tag{14c}$$

For example, consider a cloud of spherical water droplets of various sizes, so that the droplet radius r can be used as the species index k. Let $\rho(r)\mathrm{d}r$ denote the average number of droplets per unit volume with radii between r and $r + \mathrm{d}r$. Let $\sigma_s(r)$ and $\sigma_a(r)$ be the scattering and the absorption cross sections that a droplet of radius r presents to a photon, and let $f(\theta; r)$ denote the scattering angular density function for a droplet of radius r, normalized according to Eq. (10). Then Eqs. (14) take the form

$$\beta_s = \int_0^\infty \sigma_s(r)\rho(r)\mathrm{d}r, \tag{15a}$$

$$\beta = \int_0^\infty [\sigma_s(r) + \sigma_a(r)]\rho(r)\mathrm{d}r, \tag{15b}$$

$$f(\theta) = \beta_s^{-1} \int_0^\infty f(\theta; r)\sigma_s(r)\rho(r)\mathrm{d}r. \tag{15c}$$

However, in our work here we shall not make use of these formulas explicitly; instead, we shall simply assume that β_s, β, and $f(\theta)$ are given, with β_s and β any constants satisfying $0 < \beta_s \leq \beta$ and $f(\theta)$ any nonnegative function satisfying Eq. (13).

Having opted to characterize the laser radiation as a collection of photons that individually follow particlelike trajectories in the cloud, it is important that we be aware of the extent to which the wave-specific phenomenon of interference is accounted for. Interference effects in the scattering of a photon by an individual cloud particle can be fully incorporated through the function $f_k(\theta)$; e.g., for scattering from a spherical dielectric particle, interference among parts of the electromagnetic wave that travel through different regions of the sphere can be fully accounted for by taking $f_k(\theta)$ to be the corresponding Mie-scattering function, normalized according to Eq. (10). However, we have not taken into account interference effects between different cloud particles. This points up again the fact that our analysis holds only for clouds whose constituent particles are effectively uncorrelated in their spatial locations. Fortunately, virtually all not-too-dense aerosols satisfy this condition.

3. EXPRESSING J_n IN TERMS OF P_n

In this section we shall show how the function J_n in Eq. (1) is related to the laser pulse-shape function p and a carefully defined probability function P_n. The latter function will be the focus of our subsequent computational effort.

The laser pulse-shape function p is defined so that

$$N_0 p(\tau)\mathrm{d}\tau \equiv \text{average number of photons emitted by the laser in the infinitesimal time interval } (\tau, \tau + \mathrm{d}\tau). \tag{16a}$$

We assume that $p(\tau)$ is positive for $0 \leq \tau \leq \Delta$ and zero otherwise, where Δ is the pulse width; i.e., the laser pulse is emitted in the time interval $(0, \Delta)$. We also assume that p satisfies

$$\int_0^\Delta p(t)\mathrm{d}t = 1, \tag{16b}$$

so that the total number of photons in the emitted laser pulse is N_0. Most of the final results for $J_n(t)$ quoted in this paper will be for the sharp-pulse case, in which $\Delta \approx 0$ and $p(\tau) = \delta(\tau)$; however, we shall not make this sharp-pulse assumption quite yet.

We now introduce a probability function P_n, which is defined by the statement

$$P_n(t, x, y)\mathrm{d}t\mathrm{d}x\mathrm{d}y \equiv \text{probability that a photon, which is emitted by the laser at time 0, will suffer exactly } n \text{ scatterings in the cloud and then arrive at the ground in the infinitesimal time interval } (t, t + \mathrm{d}t), \text{ and in the infinitesimal area element } \mathrm{d}x\mathrm{d}y \text{ at point } (x, y), \text{ and at an angle less than } \psi_0 \text{ with the vertical.} \tag{17}$$

Notice that $P_n(t - \tau, x, y)\mathrm{d}t\mathrm{d}x\mathrm{d}y$, for $\tau < t$, is the same probability for a photon that is emitted at time τ instead of at time 0. Thus, putting

$$\iint_{\text{disk}} P_n(t - \tau, x, y)\mathrm{d}x\mathrm{d}y \equiv R_n(t - \tau), \tag{18}$$

we may infer from the addition law of probability theory that, provided that $\tau < t$,

$$R_n(t - \tau)\mathrm{d}t = \text{probability that a photon, which is emitted by the laser at time } \tau, \text{ will suffer exactly } n \text{ scatterings in the cloud and then be detected at the receiver in the infinitesimal time interval } (t, t + \mathrm{d}t)$$
$$= \text{average fraction of the } N_0 p(\tau)\mathrm{d}\tau \text{ photons emitted by the laser in } (\tau, \tau + \mathrm{d}\tau) \text{ that will suffer exactly } n \text{ scatterings in the cloud and then be detected at the receiver in } (t, t + \mathrm{d}t).$$

Therefore, provided that $t > \Delta$, the average number of photons in the laser pulse that will be scattered exactly n times in the cloud and then be detected at the receiver in $(t, t + \mathrm{d}t)$ is

$$\int_{\tau=0}^{\Delta} N_0 p(\tau)\mathrm{d}\tau \times R_n(t-\tau)\mathrm{d}t = N_0 \mathrm{d}t \int_0^{\Delta} \mathrm{d}\tau p(\tau) R_n(t-\tau).$$

If each detected photon deposits an energy ϵ in the receiver, then multiplying this last quantity by ϵ will give $J_n(t)\mathrm{d}t$, the average n-scattered radiant energy detected at the receiver in $(t, t+\mathrm{d}t)$. Thus

$$J_n(t) = N_0\epsilon \int_0^{\Delta} \mathrm{d}\tau p(\tau) R_n(t-\tau) \qquad (t > \Delta),$$

or, recalling Eq. (18),

$$J_n(t) = N_0\epsilon \int_0^{\Delta} \mathrm{d}\tau p(\tau) \iint_{\text{disk}} P_n(t-\tau, x, y)\mathrm{d}x\mathrm{d}y \qquad (t > \Delta). \quad (19)$$

Equation (19) is an exact expression for J_n in terms of p and P_n. We shall now simplify this expression by making the assumption that the receiver disk is so small that $P_n(t, x, y)$, considered as a function of x and y, is effectively constant over the disk. In that case, we can make the approximation

$$\iint_{\text{disk}} P_n(t-\tau, x, y)\mathrm{d}x\mathrm{d}y \approx \pi r_0^2 \times P_n(t-\tau, 0, 0). \quad (20a)$$

This approximation should be good provided the radius r_0 of the disk is much smaller than the shortest distance $c(t-\Delta)$ traveled by any detected photon; thus our small-disk assumption effectively imposes the requirement that

$$t \gg r_0/c + \Delta, \quad (20b)$$

or that t not be too small. Inserting approximation (20a) into Eq. (19) gives the (approximate) result

$$J_n(t) = (\pi r_0^2) N_0\epsilon \int_0^{\Delta} \mathrm{d}\tau p(\tau) P_n(t-\tau, 0, 0) \qquad [t \gg r_0/c + \Delta]. \quad (21)$$

For the remainder of this paper we shall concentrate on the sharp-pulse case, in which $\Delta \approx 0$ and $p(\tau) = \delta(\tau)$. For that case we find, using Eq. (2b), that Eq. (21) simplifies to

$$J_n(t) = (\pi r_0^2) N_0\epsilon P_n(t, 0, 0) \qquad [t \gg r_0/c, \Delta \approx 0]. \quad (22)$$

The ratio of $J_n(t)$ to $J_1(t)$, which is often all that one really requires, is then given simply by

$$J_n(t)/J_1(t) = P_n(t, 0, 0)/P_1(t, 0, 0) \qquad [t \gg r_0/c, \Delta \approx 0]. \quad (23)$$

Comparing Eqs. (21) and (22), we see that, for those cases in which the sharp-pulse approximation is not appropriate, we have to replace $P_n(t, 0, 0)$ in the preceding two formulas by $\int_0^{\Delta} \mathrm{d}\tau p(\tau) P_n(t-\tau, 0, 0)$. In either case, the problem of calculating $J_n(t)$ has now been reduced to the problem of calculating $P_n(t, 0, 0)$. Since the latter quantity is defined probabilistically [cf. Eq. (17)], there is hope of calculating it from the probabilistic laws in Eqs. (4) and (5). Such a calculation will be our goal in Sections 4–7.

4. DIRECT CALCULATION OF $P_1(t, 0, 0)$

The computation of $P_n(t, 0, 0)$ for arbitrary n is, as we shall see, a complicated and lengthy task. However, for $n = 1$ the calculation can easily be made directly from the definition in Eq. (17). That definition reads, for $n = 1$ and $x = y = 0$,

$P_1(t, 0, 0)\mathrm{d}t\mathrm{d}x\mathrm{d}y \equiv$ probability that a photon, emitted by the laser at time 0, will scatter exactly once in the cloud and then arrive, between times t and $t + \mathrm{d}t$, in the infinitesimal area element $\mathrm{d}x\mathrm{d}y$ centered on the origin. (24)

Notice that a singly scattered photon that returns infinitesimally close to the origin will necessarily do so at a declination angle less than any given value $\psi_0 > 0$, so the baffle condition in Eq. (17) is automatically satisfied here.

Figure 2 shows the path of a photon that leaves the laser at time 0, scatters once in the cloud, and then returns infinitesimally close to the origin between times t and $t + \mathrm{d}t$. In order to arrive in that time interval, it is clear from the figure that the scattering must take place on the z axis between z and $z + \mathrm{d}z$, where z and $\mathrm{d}z$ are related to t and $\mathrm{d}t$ by

$$z = ct/2 \qquad \text{and} \qquad \mathrm{d}z = c\mathrm{d}t/2. \quad (25)$$

Assuming that $z > b$, the probability that the photon reaches the point $(0, 0, z)$ without being either scattered or absorbed is, according to Eq. (4), $\exp[-\beta(z-b)]$. The subsequent probability that the photon will be scattered in the next $\mathrm{d}z$ toward the area element $\mathrm{d}x\mathrm{d}y$ at the origin is, according to Eq. (5), $\beta_s \mathrm{d}z \times f(\pi)\mathrm{d}^2\Omega$, where $\mathrm{d}^2\Omega$ is the solid angle subtended at $(0, 0, z)$ by the area element $\mathrm{d}x\mathrm{d}y$. It is seen from Fig. 2

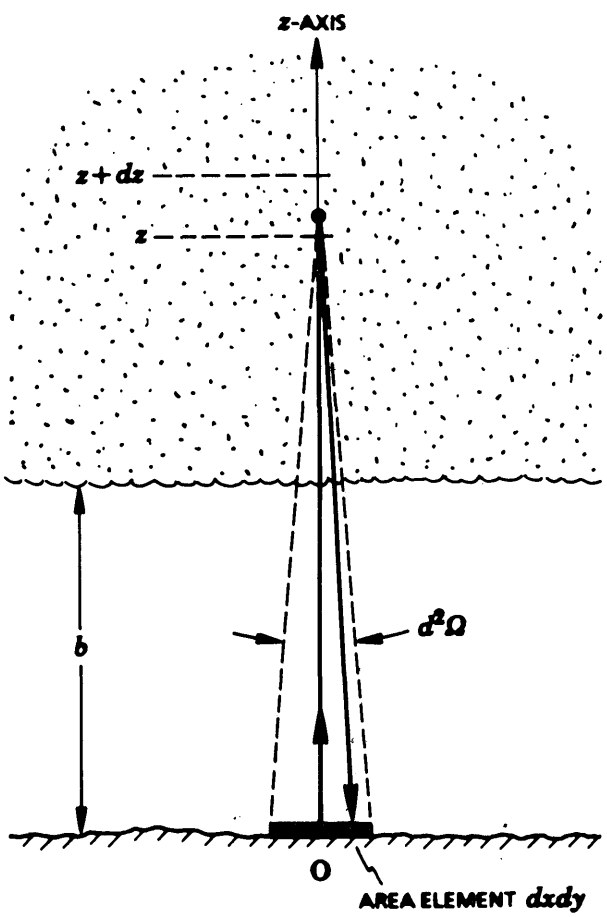

Fig. 2. Trajectory of a photon that scatters exactly once in the cloud and then returns to the ground plane infinitesimally close to the origin.

that this solid angle is given by

$$d^2\Omega = (dx\,dy)/z^2. \tag{26}$$

And finally, the probability that the photon's journey back to $dx\,dy$ will not be interrupted by a scattering or absorption is $\exp[-\beta(z-b)]$. Now, the probability in Eq. (24) is just the probability that all the foregoing events transpire; therefore the multiplication law of probability theory implies that

$$P_1(t,0,0)dt\,dx\,dy = \exp[-\beta(z-b)] \times \beta_s dz \times f(\pi)d^2\Omega \times \exp[-\beta(z-b)] \times I(z>b). \tag{27}$$

The I function here makes explicit the fact that the probability in question will be zero if z is less than b. Substituting for z, dz, and $d^2\Omega$ from Eqs. (25) and (26) and then simplifying, we conclude that

$$P_1(t,0,0) = I(ct>2b)(c\beta_s/2)(2/ct)^2 \times \exp[-\beta(ct-2b)]f(\pi). \tag{28}$$

Therefore, by using Eq. (22), we obtain for $J_1(t)$ the formula

$$J_1(t) = I(ct>2b)(\pi r_0^2)N_0\epsilon 2c\beta_s(ct)^{-2} \times \exp[-\beta(ct-2b)]f(\pi) \qquad [t \gg r_0/c,\ \Delta \approx 0]. \tag{29}$$

The fact that $P_1(t,0,0)$ in Eq. (28) diverges like t^{-2} as $t \to 0$ may at first sight be disturbing; however, this divergence does not lead to any unphysical behavior in $J_1(t)$, because the t^{-2} in Eq. (29) gets multiplied by r_0^2, and it is expressly stipulated that Eq. (29) is valid only if $r_0/t \ll c$.

5. CALCULATION OF $P_n(t, x, y)$ FOR ARBITRARY n

The calculation of $P_n(t,0,0)$ for arbitrary n is considerably longer and more circuitous than that given in the previous section for the case $n=1$. The calculation can be divided into two phases. The first phase consists of deriving a formal mathematical expression for $P_n(t,x,y)$, and the second phase consists of deducing from this formal expression a numerically computable formula for $P_n(t,0,0)$. It is worth noting that in neither phase do we have to make any approximations, so our final result is mathematically exact. The first phase involves a rather interesting combination of physical and mathematical reasoning and is detailed below in Subsection 5.A. The second phase, which is purely mathematical, is unfortunately too lengthy to present in detail in this article, so in Subsection 5.B we just mention some of the highlights and then give the final result; a complete account of the second-phase analysis may be found in a companion publication.[11]

A. Derivation of a Formal Expression for $P_n(t, x, y)$

Figure 3 illustrates the trajectory of a photon that is emitted from the origin at time 0, scatters exactly n times in the cloud, and then returns to the ground at some point $S=(x,y,0)$ (not necessarily on the receiver's disk) and at some angle ψ with the vertical. We denote the point at which the photon's ith scattering occurs by S_i $(i=1,\ldots,n)$. Identifying S_0 and S_{n+1} with the points O and S respectively, we define the $n+1$ vectors $\mathbf{u}_0, \mathbf{u}_1, \ldots, \mathbf{u}_n$ by

$$\mathbf{u}_i \equiv \mathbf{S}_i\mathbf{S}_{i+1} \equiv u_i\hat{e}_i \quad (i=0,1,\ldots,n). \tag{30}$$

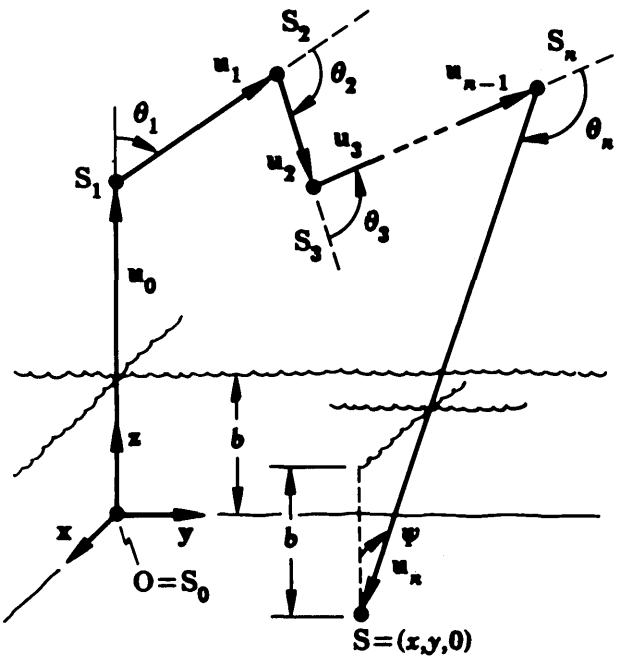

Fig. 3. Trajectory of a photon that scatters exactly n times in the cloud and then returns to the ground plane at the point $S=(x,y,0)$. The ith scattering occurs at point S_i, and the vector from S_i to S_{i+1} is denoted by $\mathbf{u}_i \equiv \hat{e}_i u_i$, where $\hat{e}_i$ is a vector of unit length.

Here, u_i denotes the magnitude of $\mathbf{u}_i$, and $\hat{e}_i$ denotes the unit vector in the direction of $\mathbf{u}_i$.

If $\hat{x}, \hat{y}$, and $\hat{z}$ are the Cartesian basis vectors of the main xyz frame, then by hypothesis,

$$\hat{e}_0 = \hat{z}. \tag{31}$$

For $i \geq 1$ we shall parameterize $\hat{e}_i$ by its polar and azimuthal angles θ_i and ϕ_i in the Cartesian frame whose basis vectors $\hat{x}_i, \hat{y}_i$, and $\hat{z}_i$ are defined according to the following recursive scheme:

$$\hat{x}_1 = \hat{x}, \qquad \hat{y}_1 = \hat{y}, \qquad \hat{z}_1 = \hat{z}, \tag{32a}$$

$$\left.\begin{aligned} \hat{z}_i &= \hat{e}_{i-1} \\ \hat{y}_i &= (\hat{z}\times\hat{e}_{i-1})/|\hat{z}\times\hat{e}_{i-1}| \\ \hat{x}_i &= \hat{y}_i \times \hat{z}_i \end{aligned}\right\}. \qquad (i=2,\ldots,n). \tag{32b}$$

With $\hat{x}_i, \hat{y}_i$, and $\hat{z}_i$ so defined, the unit vector $\hat{e}_i$ is then specified parametrically by

$$\hat{e}_i = \hat{x}_i \sin\theta_i \cos\phi_i + \hat{y}_i \sin\theta_i \sin\phi_i + \hat{z}_i \cos\theta_i \quad (i=1,\ldots,n). \tag{33}$$

Since $\hat{z}_i = \hat{e}_{i-1}$, then θ_i and ϕ_i are the canonical scattering angles of Eq. (5) for the ith scattering. The assumed azimuthal symmetry of the scattering process implies that the orientation of the x_iz_i plane is unimportant, and we have taken $\hat{y}_i \propto \hat{z}\times\hat{e}_{i-1}$ solely for convenience. Notice that, because of the recursive nature of Eqs. (32) and (33), the xyz-frame components of $\hat{e}_i$ will depend on *all* the angles $\theta_1, \phi_1, \theta_2, \phi_2, \ldots, \theta_i, \phi_i$.

The angle ψ is evidently the angle between the two unit vectors $\hat{z}$ and $-\hat{e}_n$, so

$$\cos\psi = -\hat{z}\cdot\hat{e}_n \qquad (0 \leq \psi < \pi/2). \tag{34}$$

It is clear that the trajectory of the photon in Fig. 3 is completely defined by the $n+1$ vectors $\mathbf{u}_0, \mathbf{u}_1, \ldots, \mathbf{u}_n$. However, these vectors do not form an algebraically independent set, because the stipulation that the photon return to the ground imposes the requirement that

$$0 = \hat{z} \cdot \mathbf{OS} = \hat{z} \cdot \sum_{i=0}^{n} \mathbf{u}_i = \sum_{i=0}^{n} u_i(\hat{z} \cdot \hat{e}_i).$$

This condition can be enforced by simply regarding the magnitude of the vector $\mathbf{u}_n$ to be given in terms of the other variables by the formula

$$u_n = -(\hat{z} \cdot \hat{e}_n)^{-1} \sum_{i=0}^{n-1} u_i(\hat{z} \cdot \hat{e}_i). \tag{35}$$

Therefore the trajectory of the photon in Fig. 3 can be parameterized by the $3n$ algebraically independent[14] scalar variables $u_0, \theta_1, \phi_1, u_1, \theta_2, \phi_2, \ldots, u_{n-1}, \theta_n, \phi_n$.

For the $3n$ trajectory variables just listed, we now introduce a probability function Q_n, which is defined through the statement

$Q_n(u_0, \theta_1, \phi_1, \ldots, u_{n-1}, \theta_n, \phi_n)\mathrm{d}u_0\mathrm{d}\theta_1\mathrm{d}\phi_1 \ldots \mathrm{d}u_{n-1}\mathrm{d}\theta_n\mathrm{d}\phi_n$
≡ probability that a photon, which is emitted from the laser at time 0, will scatter exactly n times in the cloud in such a way that, for each $i = 1, \ldots, n$ the free path length of the photon just before the ith scattering is between u_{i-1} and $u_{i-1} + \mathrm{d}u_{i-1}$ and its heading just after the ith scattering is in the polar solid angle $\sin\theta_i \mathrm{d}\theta_i \mathrm{d}\phi_i$ at (θ_i, ϕ_i), after which the photon returns freely to the ground at an angle less than ψ_0 with the vertical. (36)

Using Eqs. (4) and (5), along with the elementary laws of probability theory, we can write down the following exact expression for the foregoing probability:

$$\begin{aligned} &Q_n(u_0, \theta_1, \phi_1, \ldots, u_{n-1}, \theta_n, \phi_n)\mathrm{d}u_0\mathrm{d}\theta_1\mathrm{d}\phi_1 \ldots \mathrm{d}u_{n-1}\mathrm{d}\theta_n\mathrm{d}\phi_n \\ &\quad = \exp(\beta b) \times \exp[-\beta(u_n - b \sec\psi)] \\ &\qquad \times \prod_{i=1}^{n} \Bigg[\exp(-\beta u_{i-1}) \times I\Big(\hat{z} \cdot \sum_{j=0}^{i-1} \mathbf{u}_j > b\Big) \\ &\qquad \times \beta_s \mathrm{d}u_{i-1} \times f(\theta_i) \sin\theta_i \mathrm{d}\theta_i \mathrm{d}\phi_i \\ &\qquad \times I(u_{i-1} \geq 0) I(0 \leq \theta_i \leq \pi) I(0 \leq \phi_i < 2\pi) \Bigg] \\ &\qquad \times I(\cos\psi > \cos\psi_0). \end{aligned} \tag{37}$$

To justify this expression we begin by considering the quantity in braces, which refers specifically to the ith scattering. The first factor in the braces is by Eq. (4) the probability that, just before the ith scattering, the photon travels a distance u_{i-1} without being either scattered or absorbed; since for $i = 1$ this probability should read $\exp[-\beta(u_0 - b)]$ instead of $\exp(-\beta u_0)$, we place a factor $\exp(\beta b)$ outside the i product. The second factor in the braces ensures that the ith scattering occurs above cloud base; this factor simply requires the z component of the vector $\mathbf{OS}_i$ to be greater than b. The next two factors are by Eq. (5) the probability that, given the foregoing conditions, the photon is scattered in the next $\mathrm{d}u_{i-1}$ into the polar solid angle $\sin\theta_i \mathrm{d}\theta_i \mathrm{d}\phi_i$ in the direction (θ_i, ϕ_i) relative to its previous path. The last three factors in the braces simply ensure that the variables u_{i-1}, θ_i, and ϕ_i are confined to their physically accessible ranges. The product of these factors over i from 1 to n gives the probability that all these events transpire for all n scatterings. The second exponential outside the braces is, by Eq. (4), the probability that the photon is neither scattered nor absorbed after the nth scattering (note from Fig. 3 that, of the total distance u_n traveled by the photon after the nth scattering, $b \sec\psi$ is traveled outside the cloud). Finally, the I function at the end of the equation imposes the requirement that the angle ψ be less than ψ_0.

By canceling the common differentials in Eq. (37), regrouping factors, and eliminating ψ through Eq. (34), we conclude that the function Q_n defined in Eq. (36) is given by

$$\begin{aligned} &Q_n(u_0, \theta_1, \phi_1, \ldots, u_{n-1}, \theta_n, \phi_n) \\ &\quad = \beta_s{}^n \exp\Big(-\beta \sum_{i=0}^{n} u_i\Big) \exp\{\beta b[1 - (\hat{z} \cdot \hat{e}_n)^{-1}]\} \prod_{i=1}^{n} [f(\theta_i)\sin\theta_i] \\ &\qquad \times I(-\hat{z} \cdot \hat{e}_n > \cos\psi_0) \prod_{i=1}^{n} \Bigg[I\Big(\sum_{j=0}^{i-1} u_j(\hat{z} \cdot \hat{e}_j) > b\Big) \\ &\qquad \times I(u_{i-1} \geq 0) I(0 \leq \theta_i \leq \pi) I(0 \leq \phi_i < 2\pi) \Bigg]. \end{aligned} \tag{38}$$

If the ground were not present and the cloud covered all space, then we would not have to worry about distances traveled by the photon outside the cloud or scatterings occurring below cloud base; in that case, a review of the above arguments will show that Eq. (38) would still hold true, except that the exponential factor containing b and the n I functions containing b would be absent.

Our strategy is to calculate the function P_n from the function Q_n by making use of a result from the theory of random variables called the RVT theorem. This theorem can be stated as follows: Suppose that the n variables $X_1, \ldots, X_n$ are random with joint probability density function Q; this means simply that $Q(x_1, \ldots, x_n)\mathrm{d}x_1 \ldots \mathrm{d}x_n$ gives the probability that X_i will be found to have a value in the infinitesimal interval $(x_i, x_i + \mathrm{d}x_i)$, simultaneously for all $i = 1, \ldots, n$. Suppose further that the m variables $Y_1, \ldots, Y_m$ are defined by

$$Y_i = f_i(X_1, \ldots, X_n) \qquad (i = 1, \ldots, m), \tag{39a}$$

where each f_i is an ordinary real function of n real variables; this means simply that the value of Y_i is found by applying the function f_i to the simultaneous values found for $X_1, \ldots, X_n$. Then, according to the RVT theorem, the variables $Y_1, \ldots, Y_m$ are random with joint probability density function

$$\begin{aligned} P(y_1, \ldots, y_m) = &\int_{-\infty}^{\infty} \mathrm{d}x_1 \ldots \int_{-\infty}^{\infty} \mathrm{d}x_n Q(x_1, \ldots, x_n) \\ &\times \prod_{i=1}^{m} \delta[y_i - f_i(x_1, \ldots, x_n)]. \end{aligned} \tag{39b}$$

A proof of the RVT theorem may be found in Ref. 10. To see the relevance of this theorem to our problem here we first observe that, since we cannot predict with certainty the fate of a photon emitted by the laser at time 0, the variables t, x, and y in the arguments list of the function P_n and the variables $u_0, \theta_1, \phi_1, \ldots, u_{n-1}, \theta_n, \phi_n$ in the arguments list of the function Q_n are necessarily random variables.[15] Second, we note that the two functions P_n and Q_n, as defined in Eqs. (17) and (36), are *almost* the joint probability density functions for their respective variables. The qualifier here stems from the fact that the integrals of P_n and Q_n over all values of all

their variables do not equal unity, as is required of a true probability density function; however, a careful reading of Eqs. (17) and (36) will reveal that integrating P_n over all values of all its variables gives the same result as integrating Q_n over all values of all its variables, namely,

$K_n \equiv$ probability that a photon, which is emitted from the laser at time 0, will suffer exactly n scatterings in the cloud and then return freely to the ground at an angle less than ψ_0 with the vertical.

Therefore $K_n{}^{-1}P_n$ is the (properly normalized) joint probability density function for the random variables t, x, y, and $K_n{}^{-1}Q_n$ is the (properly normalized) joint probability density function for the random variables $u_0, \theta_1, \phi_1, \ldots, u_{n-1}, \theta_n, \phi_n$.

Finally, we observe that these random variables must satisfy the following three relations:

$$\sum_{i=0}^{n} u_i = ct; \qquad \hat{x} \cdot \sum_{i=0}^{n} \hat{u}_i = x; \qquad \hat{y} \cdot \sum_{i=0}^{n} \mathbf{u}_i = y. \quad (40a)$$

The first relation states that the photon's total path length is equal to its velocity times its total travel time. The last two relations state that the x and the y components of the vector **OS** (see Fig. 3) are just the corresponding coordinates of the point at which the photon returns to the ground. Viewed in a slightly different way, Eqs. (40a) imply that the random variables associated with the joint probability density function $K_n{}^{-1}P_n$ may be defined in terms of the random variables associated with the joint probability density function $K_n{}^{-1}Q_n$ through the formulas

$$t = c^{-1}\sum_{i=0}^{n} u_i; \qquad x = \sum_{i=0}^{n} u_i(\hat{x}\cdot\hat{e}_i); \qquad y = \sum_{i=0}^{n} u_i(\hat{y}\cdot\hat{e}_i). \quad (40b)$$

Therefore the RVT theorem [see Eqs. (39)] implies that

$$K_n{}^{-1}P_n(t,x,y) = \int_{-\infty}^{\infty} du_0 \ldots \int_{-\infty}^{\infty} d\phi_n \times K_n{}^{-1} Q_n(u_0, \ldots, \phi_n)\, \delta\Big(t - c^{-1}\sum_{i=0}^{n} u_i\Big) \times \delta\Big(x - \sum_{i=0}^{n} u_i(\mathbf{x}\cdot\hat{e}_i)\Big)\delta\Big(y - \sum_{i=0}^{n} u_i(\mathbf{y}\cdot\hat{e}_i)\Big). \quad (41)$$

Canceling the common factors $K_n{}^{-1}$ and inserting the expression for Q_n from Eq. (38), we get

$$P_n(t,x,y) = \beta_s{}^n \int_0^{\infty} du_0 \ldots \int_0^{\infty} du_{n-1} \int_0^{\pi} d\theta_1 \times \int_0^{2\pi} d\phi_1 \ldots \int_0^{\pi} d\theta_n \int_0^{2\pi} d\phi_n \exp\Big(-\beta\sum_{i=0}^{n} u_i\Big) \times \exp\{\beta b[1-(\hat{z}\cdot\hat{e}_n)^{-1}]\} \prod_{i=1}^{n} \Big\{f(\theta_i)\sin\theta_i \times I\Big(\sum_{j=0}^{i-1} u_j(\hat{z}\cdot\hat{e}_j) > b\Big)\Big\} I(-\hat{z}\cdot\hat{e}_n > \cos\psi_0) \times \delta\Big(t - c^{-1}\sum_{i=0}^{n} u_i\Big)\delta\Big(x - \sum_{i=0}^{n} u_i(\hat{x}\cdot\hat{e}_i)\Big) \times \delta\Big(y - \sum_{i=0}^{n} u_i(\hat{y}\cdot\hat{e}_i)\Big), \quad (42)$$

wherein we have eliminated some of the I functions in Eq. (38) by appropriately restricting the integration limits.

We recall that u_n in Eq. (42) depends on the integration variables through Eq. (35), and it is appropriate now to replace u_n with its explicit functional form. But first we make one simplification: Because of the presence of the delta function involving t, we can replace the first exponential on the right-hand side of Eq. (42) with $\exp(-\beta ct)$. That done, the variable u_n appears only in the arguments of the three delta functions, and substituting therein from Eq. (35) leads to the result

$$P_n(t,x,y) = \beta_s{}^n \exp(-\beta ct) \int_0^{\infty} du_0 \ldots \int_0^{\infty} du_{n-1} \times \int_0^{\pi} d\theta_1 \int_0^{2\pi} d\phi_1 \ldots \int_0^{\pi} d\theta_n \int_0^{2\pi} d\phi_n \times \exp\{\beta b[1-(\hat{z}\cdot\hat{e}_n)^{-1}]\} \prod_{i=1}^{n} \Big\{f(\theta_i)\sin\theta_i \times I\Big(\sum_{j=0}^{i-1} u_j(\hat{z}\cdot\hat{e}_j) > b\Big)\Big\} I(-\hat{z}\cdot\hat{e}_n > \cos\psi_0) \times \delta\Big(t - c^{-1}\sum_{i=0}^{n-1} u_i[1-(\hat{z}\cdot\hat{e}_i)(\hat{z}\cdot\hat{e}_n)^{-1}]\Big) \times \delta\Big(x - \sum_{i=0}^{n-1} u_i[(\hat{x}\cdot\hat{e}_i) - (\hat{z}\cdot\hat{e}_i)(\hat{x}\cdot\hat{e}_n)(\hat{z}\cdot\hat{e}_n)^{-1}]\Big) \times \delta\Big(y - \sum_{i=0}^{n-1} u_i[(\hat{y}\cdot\hat{e}_i) - (\hat{z}\cdot\hat{e}_i)(\hat{y}\cdot\hat{e}_n)(\hat{z}\cdot\hat{e}_n)^{-1}]\Big). \quad (43)$$

Equation (43) is an exact, formal expression for $P_n(t,x,y)$, the formality being a consequence of the delta functions in the integrand. Notice that there is a heavy implicit dependence of the integrand on the integration variables, because the quantities $(\hat{x}\cdot\hat{e}_i)$, $(\hat{y}\cdot\hat{e}_i)$, and $(\hat{z}\cdot\hat{e}_i)$ for $i \geq 1$ are all functions of the $2i$ angular variables $\theta_1, \phi_1, \ldots, \theta_i, \phi_i$. Explicit forms for those functions can be calculated recursively from Eqs. (31)–(33), but it is not necessary to go through that here.

B. Deduction of a Computable Formula for $P_n(t, 0, 0)$

The purely mathematical task of deducing from Eq. (43) a computable formula for $P_n(t,0,0)$ is unfortunately too lengthy to detail here; therefore we shall just give a brief description of the plan of the analysis and then state the principal results. A complete presentation of this phase of our calculation may be found in a companion publication.[11]

The most immediate task facing us is to integrate out analytically the three delta functions in Eq. (43) for $x = y = 0$. This task is made difficult by the circumstance that the arguments of the delta functions are not the integration variables themselves, as in Eq. (2b), but rather functions of the integration variables. To overcome this difficulty, we precede the analytical integrations with suitably chosen transformations of both the integration variables and the delta functions.[16] Thus, if we transform from the $\hat{e}_n$ polar variables (θ_n, ϕ_n) to the $\hat{e}_n$ polar variables (θ, ϕ), the latter being measured with respect to the main xyz frame, we find that we are able to transform the last two delta functions in Eq. (43) in such a way that they can be eliminated by analytically integrating over θ and ϕ. The resulting $(3n-2)$-dimensional integral contains a single delta function. For $n = 1$ it is a simple matter to eliminate that delta function by analytically

integrating over the remaining variable u_0; the result agrees exactly with Eq. (28), thus providing a reassuring check on our calculations. For $n \geq 2$ we have to proceed differently: We first transform from the $\mathbf{S}_{n-1}\mathbf{S}_n$ polar variables $(u_{n-1}, \theta_{n-1}, \phi_{n-1})$ to the $\mathbf{OS}_n$ polar variables (A_n, ψ, η). We next subject the integration variables $u_0, \ldots, u_{n-2}$ to the scaling transformations $u_i \rightarrow v_i \equiv u_i/A_n$. It is then possible to transform the remaining delta function so that it can be eliminated by analytically integrating over A_n. Finally, owing to the symmetry of the lidar backscattering problem about the z axis, we can easily make a fourth analytical integration over the azimuthal angle η of the vector $\mathbf{OS}_n$; this last integration simply produces an overall factor of 2π.

As a result of these four analytic integrations, we are left with a $(3n-4)$-dimensional integral formula for $P_n(t, 0, 0)$ in which the integration variables are

$$v_0, \ldots, v_{n-2}, \theta_1, \phi_1, \ldots, \theta_{n-2}, \phi_{n-2}, \psi.$$

Although analytically sound, the integral is not yet suitable for numerical evaluation for two reasons: First, the integration domain is unbounded, since each v_i runs from 0 to ∞. And second, the integrand is unbounded, since it contains a factor of $(1/v_{n-1})^2$. Obviously, a change of integration variables is required. The not-so-obvious key to finding a viable set of integration variables is the introduction of the set of vectors $\{\mathbf{C}_i\}$, where $\mathbf{C}_0 = \mathbf{OS}_n$ and $\mathbf{C}_i = \mathbf{S}_i\mathbf{S}_n$ for $i \geq 1$: We first change integration variables from the angles (θ_i, ϕ_i), which measure the direction of $\hat{e}_i$ relative to the polar direction $\mathbf{e}_{i-1}$, to the angles (θ_i', ϕ_i'), which measure the direction of $\hat{e}_i$ relative to the polar direction $\mathbf{C}_i$. Then we transform from the integration variable ν_i, which measures the length of $\mathbf{S}_i\mathbf{S}_{i+1}$, to the variable v_i, which measures the angle between $\mathbf{C}_{i+1}$ and the perpendicular from S_n to $\mathbf{S}_i\mathbf{S}_{i+1}$. It turns out that when $P_n(t, 0, 0)$ is expressed as an integral over the set of $(3n-4)$ variables

$$v_0, \ldots, v_{n-2}, \theta_1', \phi_1', \ldots, \theta_{n-2}', \phi_{n-2}', \theta_0' \equiv \psi,$$

both the integration domain and the integrand are bounded. Specifically, that integral is

$$P_n(t, 0, 0) = 2\pi\beta_s{}^n c(ct)^{n-3} \exp(-\beta ct) \int_0^{\psi_0} \mathrm{d}\theta_0'$$
$$\times \int_{\theta_0'-\pi/2}^{\pi/2} \mathrm{d}v_0 \left\{ \prod_{i=1}^{n-2} \int_0^{\pi} \mathrm{d}\theta_i' \int_{\theta_i'-\pi/2}^{\pi/2} \mathrm{d}\nu_i \int_0^{2\pi} \mathrm{d}\phi_i' \right\}$$
$$\times \left(\prod_{i=1}^{n-1} I(B_{i,z} > Vb/ct) \right) I(\cos\theta_0' > Vb/ct)$$
$$\times \exp[\beta b(1 + \sec\theta_0')]$$
$$\times \left(\prod_{i=1}^{n} f(\theta_i) \right) \cos\theta_0' \left\{ \prod_{i=1}^{n-2} \frac{C_i}{V} \right\} \qquad (n \geq 2), \tag{44}$$

wherein it is understood that the two products in *braces* are to be omitted in the case $n = 2$. The various quantities in the integrand of Eq. (44) are to be calculated through the following formulas, the geometric content of which is illustrated in Fig. 4 for the cases $n = 2$ through 4:

$$\begin{cases} \mathbf{C}_0 = \hat{x} \sin\theta_0' + \hat{z} \cos\theta_0', & (45a) \\ v_0 = \sin\theta_0' \tan\nu_0 + \cos\theta_0', & (45b) \\ \hat{e}_0 = \hat{z}, & (45c) \end{cases}$$

$$\begin{cases} \mathbf{C}_i = \mathbf{C}_{i-1} - v_{i-1}\hat{e}_{i-1}, & (45d) \\ v_i = C_i \sin\theta_i' \tan\nu_i + C_i \cos\theta_i', & (45e) \\ \hat{e}_i = \hat{x}e_{i,x} + \hat{y}e_{i,y} + \hat{z}e_{i,z} \quad [\text{see Eqs. (46)}] & (45f) \end{cases}$$
$$(n \geq 3; i = 1, \ldots, n-2),$$

$$\begin{cases} \mathbf{C}_{n-1} = \mathbf{C}_{n-2} - v_{n-2}\hat{e}_{n-2}, & (45g) \\ v_{n-1} = C_{n-1}, & (45h) \\ \mathbf{e}_{n-1} = \mathbf{C}_{n-1}/C_{n-1}, & (45i) \end{cases}$$

$$\mathbf{B}_1 = v_0\hat{e}_0, \tag{45j}$$

$$\mathbf{B}_i = \mathbf{B}_{i-1} + v_{i-1}\hat{e}_{i-1} \qquad (n \geq 3; i = 1, \ldots, n-1), \tag{45k}$$

$$V = 1 + \sum_{i=0}^{n-1} v_i, \tag{45l}$$

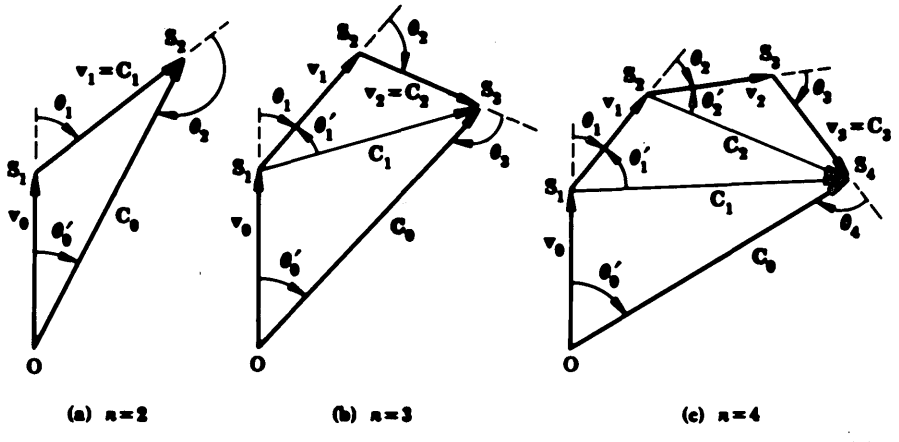

Fig. 4. Geometric interpretation of the relations among the principal variables in Eqs. (45) and (46) for (a) $n = 2$, (b) $n = 3$, and (c) $n = 4$. The photon's journey begins and ends at point O, and the ith scattering occurs at point S_i $(i = 1, \ldots, n)$. The vector $\mathbf{v}_i \equiv \mathbf{S}_i\mathbf{S}_{i+1}$ has magnitude v_i and unit direction $\hat{e}_i$. All lengths have been scaled dimensionless, with $\mathbf{OS}_n \equiv \mathbf{C}_0$ having length 1. The direction of $\hat{e}_i$ for $i \geq 1$ is measured by angles (θ_i, ϕ_i) relative to the polar axis $\mathbf{e}_{i-1}$ and by angles (θ_i', ϕ_i') relative to the polar axis $\mathbf{C}_i \equiv \mathbf{S}_i\mathbf{S}_n$. Not shown (for reasons of graphical clarity) are the vectors $\mathbf{B}_i \equiv \mathbf{OS}_i$ $(i = 1, \ldots, n-1)$ and the angles ν_i $(i = 1, \ldots, n-2)$; ν_i is the angle between $\mathbf{C}_{i+1}$ and the line perpendicular to $\mathbf{v}_i$ from S_n. The main coordinate frame is defined so that $\hat{e}_0$ points along the z axis and $\mathbf{C}_0$ lies in the xz plane. The quantity V defined in Eq. (45l) is the circumference of the (generally nonplanar) figure $\mathrm{OS}_1 \ldots \mathrm{S}_n\mathrm{O}$.

$$\theta_i = \arccos(\hat{e}_{i-1} \cdot \hat{e}_i) \qquad (i = 1, \ldots, n-1), \tag{45m}$$

$$\theta_n = \arccos(-\hat{e}_{n-1} \cdot \mathbf{C}_0). \tag{45n}$$

The components $e_{i,x}$, $e_{i,y}$, and $e_{i,z}$ in Eq. (45f) are to be calculated according to

$$\begin{bmatrix} e_{i,x} \\ e_{i,y} \\ e_{i,z} \end{bmatrix} = \begin{bmatrix} c_{i,z}c_{i,x}/c_{i,xy} & -c_{i,y}/c_{i,xy} & c_{i,x} \\ c_{i,z}c_{i,y}/c_{i,xy} & c_{i,x}/c_{i,xy} & c_{i,y} \\ -c_{i,xy} & 0 & c_{i,z} \end{bmatrix} \begin{bmatrix} \sin\theta_i' \cos\phi_i' \\ \sin\theta_i' \sin\phi_i' \\ \cos\theta_i' \end{bmatrix}$$

$$(i = 1, \ldots, n-2), \tag{46a}$$

where

$$c_{i,x} \equiv C_{i,x}/C_i, \qquad c_{i,y} \equiv C_{i,y}/C_i, \qquad c_{i,z} \equiv C_{i,z}/C_i,$$
$$c_{i,xy} \equiv (C_{i,x}{}^2 + C_{i,y}{}^2)^{1/2}/C_i, \tag{46b}$$

and where it is understood that, if $c_{i,xy} = 0$, then the 3×3 matrix in Eq. (46a) is to be taken to be the unit matrix.

Notice that Eqs. (45d), (45e), (45f), (45k), and (46) are not required if $n = 2$. The interrelated, recursive structure of the formulas for $\mathbf{C}_i$, v_i, and $\hat{e}_i$ in the above equations would obviously make the derivation of explicit formulas for those quantities quite difficult; however, explicit formulas are not required for computational methods that utilize a digital computer.

That the factor $\Pi_i(C_i/V)$ in the integrand of Eq. (44) is bounded can be seen most easily from Fig. 4: Since V is the circumference of $OS_1 \ldots S_nO$ with $OS_n \equiv C_0 = 1$, then we have $0 \le C_i/V \le 1/2$ for all i. The exponent $\beta b(1 + \sec\theta_0')$ in the integrand causes no boundedness problems when θ_0' is near $\pi/2$, because the last I function in the integrand imposes the condition that $b \sec\theta_0' < ct/V < ct$. These remarks suffice to demonstrate the boundedness of the integrand in Eq. (44). It is obvious that the integration domain is bounded; however, the dependence of the ν_i integration limits on θ_i' implies that the integration domain has a nonboxlike shape. Now, most numerical-integration methods are easier to implement if the integration domain is a unit cube. There are many transformations that will map the integration domain of Eq. (44) onto the $(3n-4)$-dimensional unit cube. We shall use the following one, which although not the simplest algebraically, has the convenient property that its Jacobian is a constant: With κ_0 defined by

$$\kappa_0 \equiv \psi_0(2\pi - \psi_0)/\pi^2, \tag{47a}$$

we define the variables p_0 and q_0 so that

$$\theta_0' = \pi[1 - (1 - \kappa_0 p_0)^{1/2}], \tag{47b}$$

$$\nu_0 = \pi[1/2 - q_0(1 - \kappa_0 p_0)^{1/2}]. \tag{47c}$$

and we define the variables p_i, q_i, and w_i for $i = 1, \ldots, n-2$ so that

$$\theta_i' = \pi(1 - p_i{}^{1/2}), \tag{47d}$$

$$\nu_i = \pi(1/2 - q_i p_i{}^{1/2}), \tag{47e}$$

$$\phi_i' = 2\pi w_i \tag{47f}$$

$(n \ge 3; i = 1, \ldots, n-2)$.

Using these formulas one can show that the integration domain in Eq. (44) maps onto the unit cube in $p_i q_i w_i$ space and also that the Jacobian of the transformation is

$$\left|\frac{\partial(\theta_0', \nu_0, \theta_1', \nu_1, \phi_1', \ldots, \theta_{n-2}', \nu_{n-2}, \phi_{n-2}')}{\partial(p_0, q_0, p_1, q_1, w_1, \ldots, p_{n-2}, q_{n-2}, w_{n-2})}\right| = \frac{\pi^{3n-4}\kappa_0}{2}. \tag{48}$$

Therefore the integral in Eq. (44) transforms under Eqs. (47) to

$$P_n(t,0,0) = \pi^{3(n-1)}\kappa_0 \beta_s{}^n c(ct)^{n-3} \exp(-\beta ct)$$
$$\times \int_0^1 dp_0 \int_0^1 dq_0 \left\{\prod_{i=1}^{n-2} \int_0^1 dp_i \int_0^1 dq_i \int_0^1 dw_i\right\}$$
$$\times \left[\prod_{i=1}^{n-1} I(B_{i,z} > Vb/ct)\right] I(\cos\theta_0' > Vb/ct)$$
$$\times \exp[\beta b(1 + \sec\theta_0')] \left[\prod_{i=1}^{n} f(\theta_i)\right] \cos\theta_0' \left\{\prod_{i=1}^{n-2} \frac{C_i}{V}\right\}$$
$$(n \ge 2). \tag{49}$$

In this, our final expression for $P_n(t,0,0)$, it is understood that the products in *braces* are to be omitted in the case $n = 2$ and also that the integrand is to be evaluated in terms of the integration variables through the formulas listed in Eqs. (45)–(47) (see also Fig. 4).

6. FINAL FORMULATION FOR $J_n(t)/J_1(t)$

In earlier sections we found that, in the sharp-pulse case and for ct much larger than the radius of the receiver's detection disk, $J_1(t)$ is given by the formula in Eq. (29), and the ratio $J_n(t)/J_1(t)$ is given by $P_n(t,0,0)/P_1(t,0,0)$. Before we divide Eq. (49) by Eq. (28), we observe that the last I function in Eq. (49) imposes the requirement that

$$ct/b > V(\cos\theta_0')^{-1} \ge V \ge 2,$$

where the last step follows from the geometry of Fig. 4. It follows that if the last I function in Eq. (49) is satisfied, then so is the I function in Eq. (28). This means that we can simply omit the I function in Eq. (28) when we divide that equation into Eq. (49). Making the division yields, after some minor algebraic simplifications, the following formulas for $n = 2$ and $n \ge 3$, respectively:

$$\frac{J_2(t)}{J_1(t)} = \frac{\pi^3\kappa_0}{2f(\pi)} (\beta_s ct) \int_0^1 dp_0 \int_0^1 dq_0 I(B_{1,z} > Vb/ct)$$
$$\times I(\cos\theta_0' > Vb/ct) \exp[\beta b(\sec\theta_0' - 1)] f(\theta_1) f(\theta_2) \cos\theta_0'$$
$$(t \gg r_0/c, \Delta \approx 0) \tag{50}$$

and

$$\frac{J_n(t)}{J_1(t)} = \frac{\pi^{3(n-1)}\kappa_0}{2f(\pi)} (\beta_s ct)^{n-1} \int_0^1 dp_0 \int_0^1 dq_0$$
$$\times \left\{\prod_{i=1}^{n-2} \int_0^1 dp_i \int_0^1 dq_i \int_0^1 dw_i\right\}$$
$$\times \left[\prod_{i=1}^{n-1} I(B_{i,z} > Vb/ct)\right] I(\cos\theta_0' > Vb/ct)$$
$$\times \exp[\beta b(\sec\theta_0' - 1)] \left[\prod_{i=1}^{n} f(\theta_i)\right] \cos\theta_0' \left\{\prod_{i=1}^{n-2} \frac{C_i}{V}\right\}$$
$$(n \ge 3; t \gg r_0/c, \Delta \approx 0). \tag{51}$$

As with Eq. (49), the integrands of Eqs. (50) and (51) are to be evaluated in terms of the integration variables through the formulas listed in Eqs. (45)–(47) (see also Fig. 4).

Equations (50) and (51) are the principal results of this paper. Given a specific functional form for $f(\theta)$ and specific numerical values for β_s, β, b, ψ_0, and t, these integral formulas can be evaluated on a digital computer using conventional numerical methods. [We shall see in the next section that, for $b = 0$ and $f(\theta) = 1/4\pi$, Eq. (50) can actually be evaluated analytically.] The conditions on t and Δ stipulated at the end of Eqs. (50) and (51) emphasize that these formulas for $J_n(t)/J_1(t)$ are valid only if ct is much larger than the radius of the receiver's disk and the emitted laser pulse is very sharp. The sharp-pulse restriction can be removed by calculating time-convolution integrals with the pulse-shape function, as was described at the end of Section 3, but the small-disk restriction cannot be removed without making substantial changes in our overall computational strategy.

Before attempting some illustrative calculations using Eqs. (50) and (51), a couple of observations are in order. First, it follows from the comment made just below the expression for Q_n in Eq. (38) that, by omitting the exponential factor and all n I functions in Eqs. (50) and (51), we have the solution to the problem of a forward-looking lidar surrounded by an infinite cloud. In that "enveloping-cloud" case, the first and the last scatterings will still be constrained to occur forward of the lidar by the conditions $v_0 > 0$ and $\theta_0' \leq \psi_0 < \pi/2$, but the $n - 2$ intermediate scatterings will be allowed to occur either forward or rearward of the lidar.

Our second observation concerns the t dependence of $J_n(t)/J_1(t)$. Notice that t in either of Eqs. (50) and (51) is confined to the factor t^{n-1} in front of the integral and to the n I functions inside the integral. In the I functions, t evidently appears in such a way that increasing t will have no effect if $b = 0$ but will weaken the I-function constraints and hence increase the value of the integral if $b > 0$. Therefore the integrals in Eqs. (50) and (51) are independent of t if $b = 0$ or if the I functions are not present, and they are increasing functions of t if $b > 0$. We conclude that

> For any given $n \geq 2$, $J_n(t)/J_1(t)$ increases with t like t^{n-1}, if $b = 0$ or if the cloud completely surrounds the lidar, and increases somewhat faster than this if $b > 0$. (52)

Of course, this does not imply that the total amount of multiply scattered radiation returning to the receiver becomes infinite as $t \to \infty$, because, as is seen from Eq. (29), $J_1(t)$ is itself tending to zero as $t \to \infty$ faster than any negative power of t.

7. AN EXAMPLE: ISOTROPIC SCATTERING IN A GROUND CLOUD AND AN ENVELOPING CLOUD

As an illustrative application of Eqs. (50) and (51), let us consider the case in which

$$f(\theta) = (4\pi)^{-1}, \qquad b = 0, \tag{53}$$

which evidently corresponds to an isotropically scattering *ground* cloud.

The isotropic-scattering function assumed in Eqs. (53) would apply if the cloud particles scattered like small, mirror-surfaced spheres. Although this is not an accurate model for light scattering from common atmospheric cloud particles, it is clearly the simplest nontrivial model possible since it has no free parameters. From the point of view of evaluating the integrals in Eqs. (50) and (51), the isotropic-scattering model is attractive because it obviates the computation of the scattering angles $\theta_1, \ldots, \theta_n$ and allows the product $f(\theta_1) \cdots f(\theta_n)$ in the integrands to be replaced by the simple constant $(4\pi)^{-n}$.

The choice of $b = 0$ in Eqs. (53) likewise produces simplifications in Eqs. (50) and (51): First, the exponential factors in the integrands are reduced to unity. Second, the right-hand sides of all the I-function inequalities become zero. The latter circumstance neatly eliminates the t dependence from the two integrals [cf. Eq. (52)]. Also, since the limits on the integration variables p_0 and q_0 already ensure through Eqs. (45)–(47) that

$$B_{1,z} = v_0 > 0, \qquad \cos\theta_0' > 0, \tag{54}$$

then the first and the last I functions in the integrands of both Eqs. (50) and (51) become unnecessary.

The conditions assumed in Eqs. (53) thus allow Eqs. (50) and (51) to be written as

$$J_n(t)/J_1(t) = K(n, \psi_0)(\beta_s ct)^{n-1}, \tag{55}$$

where the time-independent coefficients $K(n, \psi_0)$ are given by

$$K(2, \psi_0) \equiv \frac{\pi^2 \kappa_0}{8} \int_0^1 dp_0 \int_0^1 dq_0 \cos\theta_0' \tag{56}$$

and

$$K(n, \psi_0) \equiv \left(\frac{\pi^2}{4}\right)^{n-1} \frac{\kappa_0}{2} \int_0^1 dp_0 \int_0^1 dq_0 \times \left\{\prod_{i=1}^{n-2} \int_0^1 dp_i \int_0^1 dq_i \int_0^1 dw_i\right\} \times \cos\theta_0' \left[\prod_{i=1}^{n-2} I(B_{i+1,z} > 0) C_i\right] V^{-(n-2)} \qquad (n \geq 3). \tag{57}$$

In Eqs. (56) and (57), the integrands are to be evaluated in terms of the integration variables through the formulas in Eqs. (45)–(47). We note that Eq. (57) becomes identical to Eq. (56) if n is set equal to 2 and the two products over i are deleted.

In using Eqs. (55)–(57), it should be kept in mind that $J_1(t)$ is given in this case by

$$J_1(t) = N_0 \epsilon (\pi r_0^2/2\pi) c \beta_s^3 (\beta_s ct)^{-2} \exp(-\beta ct), \tag{58}$$

which follows on substituting the conditions of Eqs. (53) into Eq. (29). Also, as was discussed in Section 6, the above formulas can be made to apply to an isotropically scattering *enveloping* cloud by simply omitting the $(n - 2)$ I functions in the integrand of Eq. (57).

A. Evaluation of $K(2, \psi_0)$

The formula for $K(2, \psi_0)$ in Eq. (56) is sufficiently simple that it can be evaluated analytically. For this, it is easiest to undo

Table 1. Calculated Values of $K(n, \psi_0)$ for an Isotropically Scattering Ground Cloud[a,b]

ψ_0	n = 2	3	4	5	6
0.00001	7.8540E − 06	(3.72 ± 0.02)E − 10	—	—	—
0.00002	1.5708E − 05	(1.401 ± 0.009)E − 09	—	—	—
0.00005	3.9270E − 05	(8.06 ± 0.04)E − 09	—	—	—
0.0001	7.8539E − 05	(3.02 ± 0.02)E − 08	(1.675 ± 0.014)E − 09	(2.89 ± 0.03)E − 10	(4.83 ± 0.04)E − 11
0.0002	1.5707E − 04	(1.120 ± 0.004)E − 07	(6.72 ± 0.06)E − 09	(1.15 ± 0.01)E − 09	(1.936 ± 0.018)E − 10
0.0005	3.9267E − 04	(6.30 ± 0.02)E − 07	(4.17 ± 0.02)E − 08	(7.20 ± 0.05)E − 09	(1.211 ± 0.010)E − 09
0.001	7.8527E − 04	(2.302 ± 0.005)E − 06	(1.675 ± 0.009)E − 07	(2.88 ± 0.02)E − 08	(4.84 ± 0.04)E − 09
0.002	1.5703E − 03	(8.35 ± 0.03)E − 06	(6.67 ± 0.04)E − 07	(1.150 ± 0.007)E − 07	(1.930 ± 0.016)E − 08
0.005	3.9238E − 03	(4.52 ± 0.01)E − 05	(4.17 ± 0.02)E − 06	(7.19 ± 0.05)E − 07	(1.207 ± 0.011)E − 07
0.01	7.8414E − 03	(1.592 ± 0.003)E − 04	1.658 ± 0.009)E − 05	(2.88 ± 0.02)E − 06	(4.83 ± 0.04)E − 07
0.02	1.5657E − 02	(5.52 ± 0.01)E − 04	(6.58 ± 0.003)E − 05	(1.149 ± 0.007)E − 05	(1.938 ± 0.017)E − 06
0.05	3.8941E − 02	(2.753 ± 0.005)E − 03	(4.00 ± 0.02)E − 04	(7.13 ± 0.04)E − 05	(1.207 ± 0.010)E − 05
0.1	7.7162E − 02	(8.92 ± 0.002)E − 03	(1.527 ± 0.011)E − 03	(2.82 ± 0.02)E − 04	(4.79 ± 0.04)E − 05
0.2	1.5108E − 01	(2.747 ± 0.004)E − 02	(5.60 ± 0.04)E − 03	(1.088 ± 0.007)E − 03	(1.872 ± 0.014)E − 04
0.4	2.8664E − 01	(7.72 ± 0.01)E − 02	(1.865 ± 0.012)E − 02	(3.90 ± 0.02)E − 03	(6.88 ± 0.05)E − 04
0.6	4.0244E − 01	(1.315 ± 0.002)E − 01	(3.49 ± 0.02)E − 02	(7.51 ± 0.05)E − 03	(1.367 ± 0.010)E − 03
0.8	4.9576E − 01	(1.812 ± 0.002)E − 01	(5.05 ± 0.03)E − 02	(1.122 ± 0.007)E − 02	(2.08 ± 0.02)E − 03
1.0	5.6545E − 01	(2.212 ± 0.003)E − 01	(6.40 ± 0.04)E − 02	(1.448 ± 0.009)E − 02	(2.69 ± 0.02)E − 03
1.2	6.1182E − 01	(2.488 ± 0.003)E − 01	(7.32 ± 0.05)E − 02	(1.68 ± 0.01)E − 02	(3.14 ± 0.03)E − 03
1.4	6.3657E − 01	(2.637 ± 0.004)E − 01	(7.82 ± 0.06)E − 02	(1.80 ± 0.01)E − 02	(3.36 ± 0.03)E − 03
1.5707	6.4270E − 01	(2.674 ± 0.004)E − 01	(7.96 ± 0.06)E − 02	(1.83 ± 0.01)E − 02	(3.47 ± 0.03)E − 03

[a] The computer "E-notation" is used; e.g., 7.5E − 08 means 7.5×10^{-8}.
[b] The figures in column 2 are from Eq. (60). The figures in columns 3 through 6 were obtained by Monte Carlo integrating Eq. (57). The stated uncertainties represent 99% confidence limits (i.e., 2.58 standard deviations).

Table 2. Calculated Values of $K(n, \psi_0)$ for an Isotropically Scattering Enveloping Cloud[a,b]

ψ_0	n = 2	3	4	5	6
0.00001	7.8540E − 06	(3.73 ± 0.03)E − 10	—	—	—
0.00002	1.5708E − 05	(1.409 ± 0.009)E − 09	—	—	—
0.00005	3.9270E − 05	(8.08 ± 0.04)E − 09	—	—	—
0.0001	7.8539E − 05	(3.03 ± 0.02)E − 08	(1.785 ± 0.009)E − 09	(3.35 ± 0.02)E − 10	(6.12 ± 0.06)E − 11
0.0002	1.5707E − 04	(1.126 ± 0.004)E − 07	(7.13 ± 0.04)E − 09	(1.336 ± 0.007)E − 09	(2.45 ± 0.02)E − 10
0.0005	3.9267E − 04	(6.32 ± 0.02)E − 07	(4.45 ± 0.02)E − 08	(8.36 ± 0.05)E − 09	(1.53 ± 0.01)E − 09
0.001	7.8527E − 04	(2.317 ± 0.007)E − 06	(1.79 ± 0.01)E − 07	(3.35 ± 0.02)E − 08	(6.15 ± 0.05)E − 09
0.002	1.5703E − 03	(8.42 ± 0.03)E − 06	(7.16 ± 0.04)E − 07	(1.340 ± 0.009)E − 07	(2.44 ± 0.02)E − 08
0.005	3.9238E − 03	(4.56 ± 0.01)E − 05	(4.47 ± 0.02)E − 06	(8.35 ± 0.05)E − 07	(1.52 ± 0.01)E − 07
0.01	7.8414E − 03	(1.608 ± 0.003)E − 04	1.776 ± 0.009)E − 05	(3.35 ± 0.02)E − 06	(6.09 ± 0.05)E − 07
0.02	1.5657E − 02	(5.58 ± 0.01)E − 04	(7.02 ± 0.03)E − 05	(1.335 ± 0.007)E − 05	(2.46 ± 0.02)E − 06
0.05	3.8941E − 02	(2.792 ± 0.004)E − 03	(4.28 ± 0.02)E − 04	(8.30 ± 0.04)E − 05	(1.53 ± 0.01)E − 05
0.1	7.7162E − 02	(9.08 ± 0.01)E − 03	(1.645 ± 0.011)E − 03	(3.28 ± 0.02)E − 04	(6.09 ± 0.04)E − 05
0.2	1.5108E − 01	(2.805 ± 0.004)E − 02	(6.05 ± 0.04)E − 03	(1.273 ± 0.007)E − 03	(2.38 ± 0.02)E − 04
0.4	2.8664E − 01	(7.963 ± 0.009)E − 02	(2.04 ± 0.01)E − 02	(4.61 ± 0.03)E − 03	(8.81 ± 0.06)E − 04
0.6	4.0244E − 01	(1.367 ± 0.002)E − 01	(3.87 ± 0.02)E − 02	(9.05 ± 0.05)E − 03	(1.78 ± 0.01)E − 03
0.8	4.9576E − 01	(1.899 ± 0.002)E − 01	(5.71 ± 0.03)E − 02	(1.384 ± 0.007)E − 02	(2.78 ± 0.02)E − 03
1.0	5.6545E − 01	(2.335 ± 0.002)E − 01	(7.30 ± 0.04)E − 02	(1.806 ± 0.009)E − 02	(3.68 ± 0.03)E − 03
1.2	6.1182E − 01	(2.647 ± 0.003)E − 01	(8.51 ± 0.05)E − 02	(2.13 ± 0.01)E − 02	(4.39 ± 0.03)E − 03
1.4	6.3657E − 01	(2.821 ± 0.003)E − 01	(9.21 ± 0.06)E − 02	(2.34 ± 0.01)E − 02	(4.80 ± 0.03)E − 03
1.5707	6.4270E − 01	(2.865 ± 0.004)E − 01	(9.36 ± 0.06)E − 02	(2.37 ± 0.01)E − 02	(4.91 ± 0.04)E − 03

[a] The computer "E-notation" is used; e.g., 7.5E − 08 means 7.5×10^{-8}.
[b] The figures in column 2 are from Eq. (60). The figures in columns 3 through 6 were obtained by Monte Carlo integrating Eq. (57), omitting the two i products; the uncertainties represent 99% confidence limits (i.e., 2.58 standard deviations).

the cubing transformation of Eqs. (47) and recover the integration variables θ_0' and ν_0. Since Eqs. (47b) and (47c) map the unit square in the p_0q_0 plane onto the region $\{(\theta_0', \nu_0) \| 0 \le \theta_0' \le \psi_0, \theta_0' - \pi/2 \le \nu_0 \le \pi/2\}$ with [see Eq. (48)]

$$d\theta_0' d\nu_0 = (\pi^2\kappa_0/2) dp_0 dq_0,$$

then Eq. (56) is the same as

$$K(2, \psi_0) \equiv \frac{1}{4} \int_0^{\psi_0} d\theta_0' \int_{\theta_0'-\pi/2}^{\pi/2} d\nu_0 \cos\theta_0'. \quad (59)$$

The ν_0 integration is trivial, and the subsequent θ_0' integration is easily accomplished by parts:

$$\begin{aligned} K(2, \psi_0) &= \frac{1}{4} \int_0^{\psi_0} d\theta_0' \cos\theta_0' \left[\frac{\pi}{2} - \left(\theta_0' - \frac{\pi}{2}\right)\right] \\ &= \frac{1}{4} \int_0^{\psi_0} (\pi - \theta_0') \cos\theta_0' d\theta_0' \\ &= \frac{1}{4} \left[(\pi - \theta_0') \sin\theta_0' \Big|_0^{\psi_0} - \int_0^{\psi_0} \sin\theta_0' (-d\theta_0')\right]. \end{aligned}$$

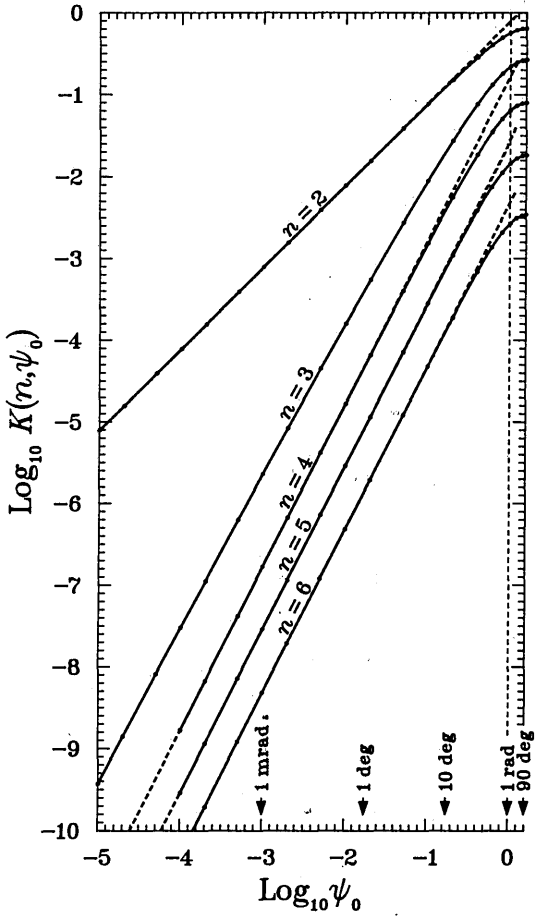

Fig. 5. A plot of $\log_{10} K(n, \psi_0)$ versus $\log_{10} \psi_0$ for $n = 2, 3, \ldots, 6$ for an isotropically scattering *ground* cloud. The plotted points are from the data in Table 1, which in turn were obtained from Eq. (60) for $n = 2$ and from Monte Carlo evaluations of Eq. (57) for $n = 3, \ldots, 6$. The solid curves are smooth interpolations through the data points. The dashed lines over the $n = 2, 4, 5, 6$ curves are plots of the estimated small-angle asymptotes in Eqs. (65); the $n = 3$ curve does not appear to have a small-angle constant-slope asymptote, evincing instead the logarithmic behavior of expression (67).

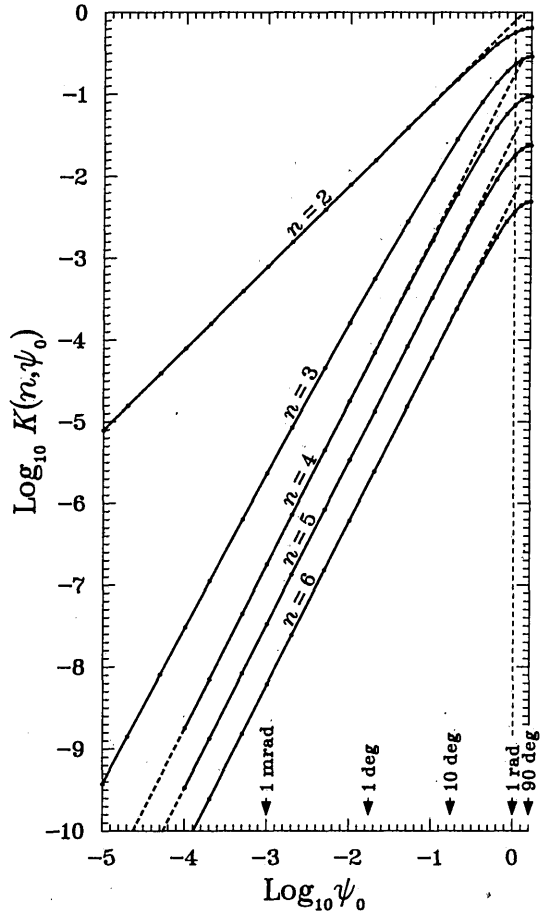

Fig. 6. A plot of $\log_{10} K(n, \psi_0)$ versus $\log_{10} \psi_0$ for $n = 2, 3, \ldots, 6$ for an isotropically scattering *enveloping* cloud. The plotted points are from the data in Table 2, which in turn were obtained from Eq. (60) for $n = 2$ and from Monte Carlo evaluations of Eq. (57), without the I functions, for $n = 3, \ldots, 6$. The full curves are smooth interpolations through the data points. The dashed lines over the $n = 2, 4, 5, 6$ curves are plots of the estimated small-angle asymptotes in expressions (66); the $n = 3$ curve does not appear to have a small-angle constant-slope asymptote, evincing instead the logarithmic behavior of expression (67).

Thus

$$K(2, \psi_0) = (1/4)[(\pi - \psi_0)\sin\psi_0 + (1 - \cos\psi_0)]. \quad (60)$$

Numerical values of $K(2, \psi_0)$ for ψ_0 between 10^{-5} and $\pi/2$ rad are tabulated in Tables 1 and 2 and plotted in Figs. 5–7.

B. Evaluation of $K(n, \psi_0)$ for $n \ge 3$

Since the integral expression for $K(n, \psi_0)$ in Eq. (57) is fivefold, eightfold, elevenfold, ... for $n = 3, 4, 5, \ldots$, an evaluation by numerical methods seems unavoidable. We shall use here the Monte Carlo integration method [see, for example, Ref. 17]. Equation (57) says that $K(n, \psi_0)$ is the integral of the function

$$F = \left(\frac{\pi^2}{4}\right)^{n-1} \frac{\kappa_0}{2} \cos\theta_0' \left(\prod_{i=1}^{n-2} I(B_{i+1,z} > 0) C_i\right) V^{-(n-2)} \quad (61)$$

over the unit cube in the space of the $3n - 4$ variables $p_0, q_0, p_1, q_1, w_1, \ldots, p_{n-2}, q_{n-2}, w_{n-2}$. The Monte Carlo method of evaluating Eq. (57) is based on the fact that this integral can also be regarded as the average of F with respect to the uni-

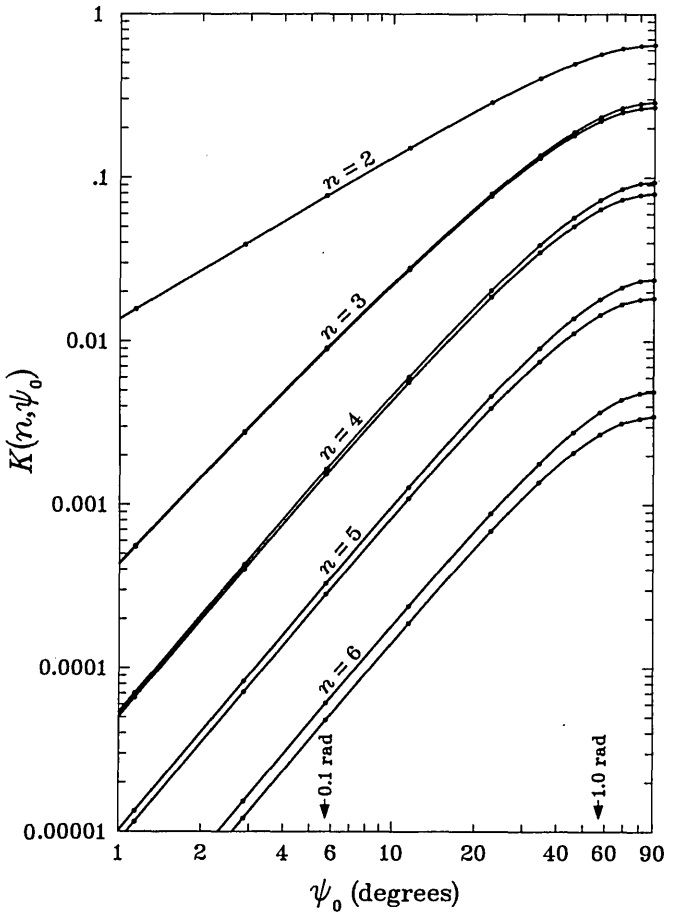

Fig. 7. A log–log scale plot of $K(n, \psi_0)$ versus ψ_0 for $n = 2, 3, \ldots, 6$ for an isotropically scattering ground cloud (lower curve for each n) and an isotropically scattering enveloping cloud (upper curve for each n). This plot is essentially a superposition of portions of Figs. 5 and 6 for which $\psi_0 \geq 1°$.

form random distribution on that unit cube. The method is implemented by first generating N random points uniformly inside the $(3n-4)$-dimensional unit cube in (pqw) space and then calculating the two quantities

$$\langle F\rangle_N \equiv \frac{1}{N}\sum_{i=1}^{N} F(i), \qquad \langle F^2\rangle_N \equiv \frac{1}{N}\sum_{i=1}^{N} [F(i)]^2, \quad (62a)$$

where $F(i)$ is the value of F at the ith random point. The central limit theorem then tells us that, provided that N is taken sufficiently large,

$$K(n, \psi_0) \approx \langle F\rangle_N \pm a[\langle F^2\rangle_N - \langle F\rangle_N{}^2]^{1/2} N^{-1/2}, \quad (62b)$$

where the $\pm$ uncertainty represents confidence limits of 68.3% if $a = 1$, 95.5% if $a = 2$, 99.0% if $a = 2.58$, and 99.7% if $a = 3$. Since $\langle F\rangle_N$ and $\langle F^2\rangle_N$ are asymptotically independent of N, the uncertainty in the Monte Carlo estimate decreases as $N^{-1/2}$ with increasing N; for integrals of dimensionality greater than about 4 this is a faster rate of convergence with the number of computation points that can be obtained with classical quadrature methods.

A FORTRAN program entitled ISOSCAT1 was written to carry out the calculations required by Eq. (61) and expressions (62) for arbitrary input values of $n (n \geq 2)$, ψ_0 $(0 < \psi_0 < \pi/2)$, and N. An additional input variable to ISOSCAT1 gives the user the option of deleting the $(n-2)$ I functions in Eq. (61), an action that changes the problem from an isotropically scattering *ground* cloud to an isotropically scattering *enveloping* cloud. Test runs of ISOSCAT1 with $n = 2$ [for which the product over i in Eq. (61) is simply omitted] were found to give results in complete agreement with the formula in Eq. (60), thus providing a limited but reassuring check on the validity of the program.

A total of 75 runs of ISOSCAT1 were made for the ground-cloud case with values of n ranging from 3 to 6 and values of ψ_0 ranging from 10^{-5} to $\pi/2$. These runs were then repeated for the enveloping-cloud case. The results are tabulated in Tables 1 and 2 and are plotted with smooth ψ_0 interpolations in Figs. 5–7. The uncertainties quoted in the tables were computed in accordance with expression (62b) with $a = 2.58$ and therefore represent 99% confidence limits. In the plots of Figs. 5–7, these 99% confidence limits are in all cases smaller than the size of the plotted points.

It should be mentioned that, in obtaining most of the entries in Tables 1 and 2, program ISOSCAT1 employed a Monte Carlo variance-reducing technique known as importance sampling.[17] When successful, this technique reduces the asymptotic value of $\langle F^2\rangle_N$ without changing the asymptotic value of $\langle F\rangle_N$, thus producing a smaller uncertainty in expression (62b) for the same value of N. The specific action taken by ISOSCAT1 in these calculations was to importance-sample the variable q_0 according to a symmetric split-Cauchy distribution whenever ψ_0 was less than 1 rad; this action was found to increase the efficiency of the Monte Carlo calculations by factors ranging from 1 to 1000, depending on the values of ψ_0 and n.

The figures cited in Tables 1 and 2 were obtained by running program ISOSCAT1 on a Sperry (Univac) 1100/83 computer. As with most Monte Carlo integration programs, ISOSCAT1 requires relatively little memory storage but a great deal of number-crunching ability. The following remarks are intended to convey some idea of the computing power utilized in obtaining the figures in Tables 1 and 2: Each $K(3, n)$ value was computed with $N = 2 \times 10^6$ points and required approximately 30 min of CPU time; the value for $K(4, 0.1)$ was computed with $N = 2 \times 10^5$ points and required approximately 5 min of CPU time; the value for $K(6, 0.0001)$ was computed with $N = 1.1 \times 10^6$ points and required approximately 40 min of CPU time. Based on benchmark runs of ISOSCAT1 on other computers, these CPU times would have been larger by a factor of about 3 for running on a VAX 11/780 computer and smaller by a factor of about 1/3 for running on a Cray X-MP computer. Since the uncertainty in a Monte Carlo result is inversely proportional to the square root of N, and hence also inversely proportional to the square root of the run time, the CPU times quoted above could have been considerably reduced at the expense of slightly larger uncertainties or weaker confidence limits; thus, for example, if we were willing to accept uncertainties twice as large as those quoted above, the corresponding CPU times could have been reduced by a factor of 1/4. We chose to be somewhat conservative in this regard.

C. Assessing the Results

Figure 5 is a plot of $\log_{10} K(n, \psi_0)$ versus $\log_{10} \psi_0$ for the isotropically scattering ground-cloud data given in Table 1. Fig. 6 is a like plot for the isotropically scattering enveloping-cloud data given in Table 2. The portions of Figs. 5 and 6 corre-

sponding to ψ_0 between 1° and 90° are plotted together on log–log axes in Fig. 7: There, each n value applies to two curves, the upper curve being for the enveloping-cloud case and the lower curve being for the ground-cloud case.

These results show that $K(n, \psi_0)$ is generally a monotonically decreasing function of n for fixed ψ_0 and a monotonically increasing function of ψ_0 for fixed n. Figure 7 shows that the difference between the enveloping-cloud and the ground-cloud values of $K(n, \psi_0)$ for $n \geq 3$ increases smoothly with increasing n and increasing ψ_0, but, aside from that, the enveloping-cloud and the ground-cloud results are rather similar. Notice, in particular, that the enveloping-cloud and the ground-cloud values for $K(3, \psi_0)$ are practically identical for small ψ_0.

Considerable effort was devoted to examining the behavior of $K(n, \psi_0)$ for small ψ_0. If $\sin\psi_0$ and $\cos\psi_0$ in Eq. (60) are replaced by their small-angle approximations, Eq. (60) reduces to

$$K(2, \psi_0) \approx (\pi/4)\psi_0 \qquad (\psi_0 \ll 1). \tag{63a}$$

Therefore

$$\log K(2, \psi_0) \approx \log(\pi/4) + \log\psi_0, \qquad (\psi_0 \ll 1) \tag{63b}$$

which shows that a plot of $\log K(2, \psi_0)$ versus $\log\psi_0$ for $\psi_0 \ll 1$ will be a straight line with slope 1 and $\log K$ intercept of $\log(\pi/4)$; this line is plotted as a dashed line over the $n = 2$ curves in Figs. 5 and 6. More generally, if

$$y = ax^b,$$

then

$$\log y = \log a + b \log x, \tag{64}$$

showing that a plot of $\log y$ versus $\log x$ will be a straight line with slope b and $\log y$ intercept of $\log a$. For the data plotted in both Figs. 5 and 6, it was found possible to fit the small-angle portions of the $n = 4, 5, 6$ curves with straight lines of slope 2, thus implying that, for $n = 4, 5, 6$, $K(n, \psi_0)$ tends to zero with ψ_0 like ψ_0^2. The dashed lines over the $n = 4, 5, 6$ curves in Figs. 5 and 6 are the best-fit small-angle asymptotes with slope $b = 2$. Equations (64) imply that the a values for these asymptotes can be read off from their intercepts with the line $\log_{10}\psi_0 = 0$, which line is also shown dashed in Figs. 5 and 6. In this way we have deduced the following small-angle approximations to $K(n, \psi_0)$ for $n = 2, 4, 5, 6$:

Ground-cloud case, $\psi_0 \ll 1$:

$$K(2, \psi_0) \approx 0.7854 \times \psi_0, \tag{65a}$$

$$K(4, \psi_0) \approx 0.1673 \times \psi_0^2, \tag{65b}$$

$$K(5, \psi_0) \approx 0.0288 \times \psi_0^2, \tag{65c}$$

$$K(6, \psi_0) \approx 0.00483 \times \psi_0^2. \tag{65d}$$

Enveloping-cloud case, $\psi_0 \ll 1$:

$$K(2, \psi_0) \approx 0.7854 \times \psi_0, \tag{66a}$$

$$K(4, \psi_0) \approx 0.1785 \times \psi_0^2, \tag{66b}$$

$$K(5, \psi_0) \approx 0.0335 \times \psi_0^2, \tag{66c}$$

$$K(6, \psi_0) \approx 0.00613 \times \psi_0^2. \tag{66d}$$

Conspicuously absent from approximations (65) and (66) are small-angle power-law formulas for $K(3, \psi_0)$. In fact, neither of the $n = 3$ curves in Figs. 5 and 6 can be well fitted by a small-angle asymptote of constant slope. However, a moderately good small-angle fit can be provided by the algebraic form $-C\psi_0^2 \ln\psi_0$, whose log–log slope, $2 + (1/\ln\psi_0)$, approaches 2 from below as $\psi_0 \downarrow 0$. Specifically, we find that for both the ground-cloud and the enveloping-cloud cases, our results can be approximated by

$$K(3, \psi_0) \approx -0.33 \times \psi_0^2 \ln\psi_0 = 0.33 \times \psi_0^2 \ln(1/\psi_0) \qquad (10^{-5} \leq \psi_0 \leq 10^{-3}). \tag{67}$$

Of course, this formula, like the above formulas for $n \geq 4$, must be regarded as essentially empirical at this point. But the conclusion that $K(3, \psi_0)$ does not approach zero with ψ_0 as an integer power of ψ_0 seems inescapable and constitutes a rather surprising result. It implies, for instance, that $K(3, \psi_0)$ does not have a Taylor series expansion in ψ_0 about $\psi_0 = 0$.

Now let us examine the implications of these calculated values of $K(n, \psi_0)$ for the physically significant quantity $J_n(t)/J_1(t)$, as given in Eq. (55). For this it is convenient to introduce the dimensionless variable

$$z^* \equiv \beta_s ct/2. \tag{68}$$

Physically, z^* can be interpreted as the scattering altitude, in multiples of β_s^{-1}, of singly scattered photons arriving at the receiver at time t. We also introduce the quantity

$$J_n^*(z^*) \equiv J_n(t) \equiv J_n(2z^*/\beta_s c), \tag{69}$$

which is evidently the n-scattered power measured at the receiver at the instant when the scattering altitude of co-arriving once-scattered photons equals $z^* \times \beta_s^{-1}$. Combining Eqs. (69), (55), and (68), we get

$$J_n^*(z^*)/J_1^*(z^*) = [2^{n-1}K(n, \psi_0)](z^*)^{n-1}. \tag{70a}$$

Taking logarithms of both sides gives

$$\log[J_n^*(z^*)/J_1^*(z^*)] = \log[2^{n-1}K(n, \psi_0)] + (n-1)\log z^*. \tag{70b}$$

Therefore, a log–log scale plot of $J_n^*(z^*)/J_1^*(z^*)$ versus z^* will be a straight line with slope $(n-1)$ and ordinate-axis intercept $2^{n-1}K(n, \psi_0)$. In Fig. 8 we show such plots for the ground-cloud case with receiver-aperture half-angles of 0.001, 0.01, 0.1, and $\pi/2$ rad. We see from these figures that, for $z^* \leq 1$, it is *always* the case that $J_2^*(z^*) > J_3^*(z^*) > J_4^*(z^*) > \ldots$, and it is *usually* the case that $J_1^*(z^*) > J_2^*(z^*)$. However, the latter inequality can be violated if ψ_0 is sufficiently large; for example, we note from Fig. 8(d) that, at $\psi_0 = \pi/2$, both $J_2^*(1)$ and $J_3^*(1)$ exceed $J_1^*(1)$. As z^* increases above 1, the situation becomes quite complicated, with higher orders of multiply scattered radiation rapidly overtaking the singly scattered radiation, and also with the relative predominance of the various multiple-scattering intensities becoming strongly dependent on z^* and ψ_0; for example, for $\psi_0 = 0.1$ [see Fig. 8(c)], we have at $z^* = 4$ the ordering $J_6 > J_5 > J_1 > J_4 > J_2 > J_3$. The general lesson to be learned here is that the usual supposition (or hope) that $J_n(t) \gg J_{n+1}(t)$ is not necessarily true for times t corresponding to single-scattering altitudes greater than or on the order of β_s^{-1}.

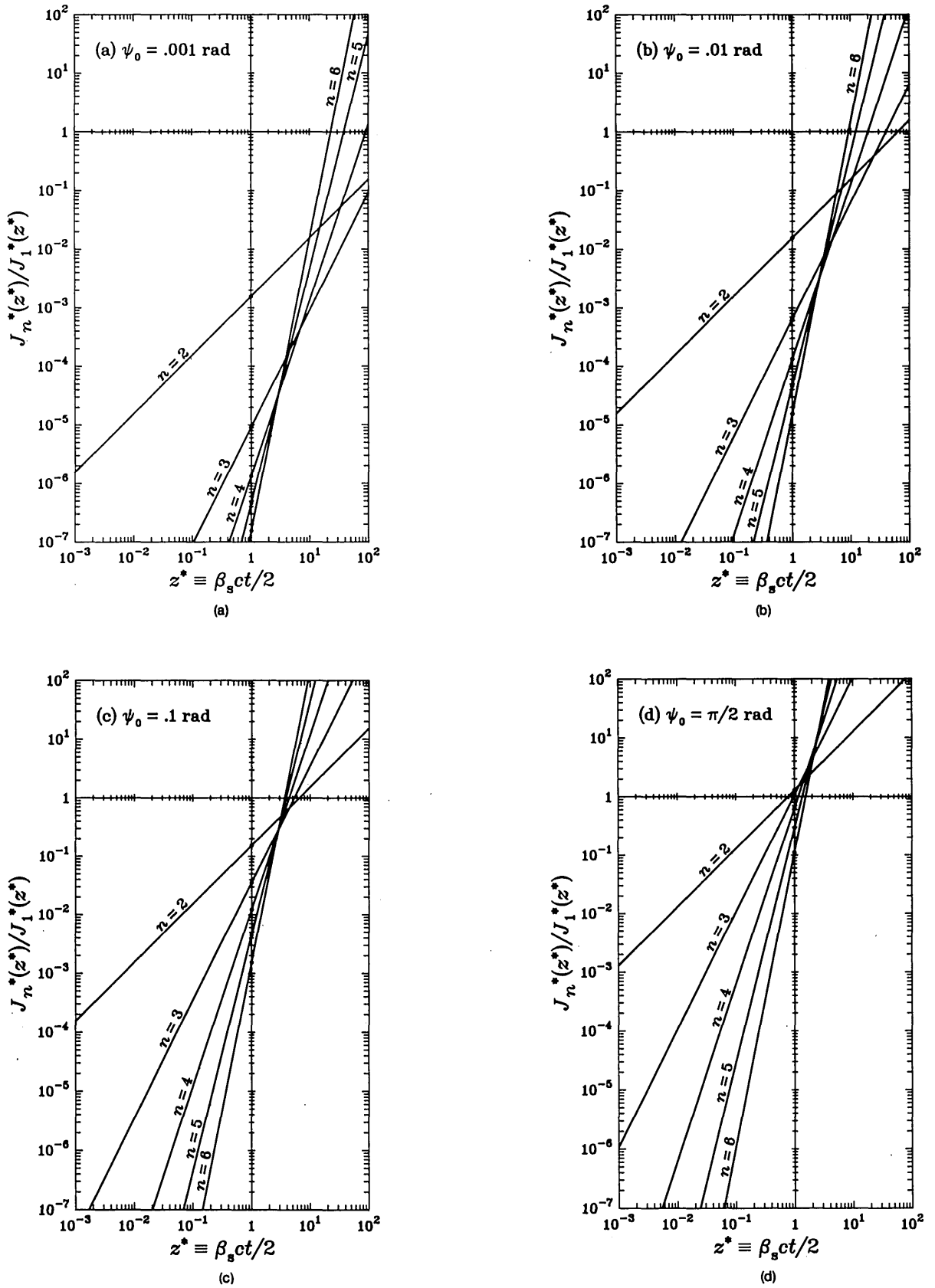

Fig. 8. Log–log scale plots of $J_n^*(z^*)/J_1^*(z^*)$ versus $z^* \equiv \beta_s ct/2$ for $n = 2, 3, \ldots, 6$ for an isotropically scattering ground cloud with (a) $\psi_0 = 0.001$ rad, (b) $\psi_0 = 0.01$ rad, (c) $\psi_0 = 0.1$ rad, and (d) $\psi_0 = \pi/2$ rad. Physically, $J_n^*(z^*)$ is the n-scattered radiation power measured at the receiver at the moment when the scattering altitude of co-arriving singly scattered radiation equals $z^* \times \beta_s^{-1}$. The curves are plots of Eqs. (70), using the $K(n, \psi_0)$ values from Table 1.

8. SUMMARY

In this paper we have shown how the time-dependent lidar multiple-backscattering problem can be rigorously analyzed by using the theory of random variables—a theory that seems especially well suited to this intrinsically probabilistic problem. We began by deriving the stochastic propagation laws for a photon in a well-mixed cloud [see Eqs. (4) and (5)] and showing how the parameters β_s, β, and f contained in those laws can be calculated in terms of the physical properties of the cloud [see Eqs. (14) and (15)]. We next showed how $J_n(t)$, the nth-order backscattered power measured by the receiver at a time t after the laser fired, may be expressed in terms of a certain probability function $P_n(t, 0, 0)$ [see Eqs. (21)–(23)]. Formulas for $P_1(t, 0, 0)$ and $J_1(t)$ were readily computed [see Eqs. (28) and (29)], but the problem for $n \geq 2$ proved to be much more difficult. After a lengthy analysis, which however entailed no approximations, we finally obtained a tractable expression for $P_n(t, 0, 0)$ for general n in terms of the cloud base height b, the receiver-aperture half-angle ψ_0, and the cloud parameters β_s, β, and f [see Eq. (49)]. Our final formula for $J_n(t)/J_1(t)$ for $n \geq 2$ is in the form of a $(3n - 4)$-dimensional definite integral with a bounded integrand and a bounded-integration domain [see Eqs. (50) and (51) and also Eq. (29)].

Our derived formula for $J_n(t)/J_1(t)$ ignores polarization effects and is otherwise subject to the restrictions that the cloud be well mixed, that the initial laser beam be narrow and well collimated, that the receiver be very small, and that the pulse duration be very short. A procedure was given to circumvent, if desired, the short-pulse restriction. We should note that the small-receiver condition usually obtains in practical applications and actually causes serious efficiency problems for Monte Carlo simulation schemes. A noteworthy feature of our derivation is that, although it is lengthy, it requires no approximations that do not follow easily from the aforementioned assumptions; i.e., given the above restrictions, our formula for $J_n(t)/J_1(t)$ is exact.

As an illustrative application of our formula for $J_n(t)/J_1(t)$, we evaluated it for $n = 2$ through 6 for an idealized cloud of isotropically scattering particles (f = constant); we considered specifically the ground-cloud ($b = 0$) and the enveloping-cloud ($b = -\infty$) cases. For $n = 2$ an explicit analytic formula was obtained [see Eqs. (55) and (60)]; for $n = 3$ through 6, numerical results were obtained by performing Monte Carlo integrations [see Eq. (55) and Figs. 5 and 6]. Particular attention was given to the important case in which ψ_0 is very small [see Eqs. (65)–(67)]. These model calculations, although not applicable to naturally occurring clouds, do demonstrate that our integral formula for $J_n(t)$ is computationally feasible. Unfortunately, no means of verifying the numerical results obtained here is readily at hand, so their correctness is for now contingent solely on no mistakes having been made in either our analysis or our computer work. However, the author is currently developing an entirely independent computational scheme for the enveloping-cloud case when $n \gg 1$, which should provide a check on the correctness of the numerical results reported here. That work, as well as applications of our present formula to more-realistic (nonisotropic) angular scattering functions f, will be reported on in subsequent publications.

ACKNOWLEDGMENTS

The author is grateful to members of the Naval Weapons Center's Central Computing Facility for their assistance in running program ISOSCAT1. Special thanks are due to H. L. Lindblom for his help in using the DISSPLA graphics software and associated hardware to produce the data plots. This research was funded jointly by the Atmospheric Sciences Program of the U.S. Air Force Office of Scientific Research and the Independent Research Program of the Naval Weapons Center.

REFERENCES

1. S. Chandrasekhar, *Radiative Transfer* (Dover, New York, 1960).
2. K. N. Liou and R. M. Schotland, "Multiple backscattering and depolarization from water clouds for a pulsed lidar system," J. Atmos. Sci. **28**, 772–784 (1971).
3. E. W. Eloranta, "Calculation of doubly scattered lidar returns," Ph.D. dissertation (University of Wisconsin, Madison, Wisconsin, 1972).
4. J. A. Weinman, "Effects of multiple scattering on light pulses reflected by turbid atmospheres," J. Atmos. Sci. **33**, 1763–1771 (1976).
5. L. L. Carter, H. G. Horak, and M. T. Sandford II, "An adjoint Monte Carlo treatment of the equations of radiative transfer for polarized light," J. Comput. Phys. **26**, 119–138 (1978).
6. Q. Cai and K. N. Liou, "Theory of time-dependent multiple backscattering from clouds," J. Atmos. Sci. **38**, 1452–1466 (1981).
7. G. N. Plass and G. W. Kattawar, "Reflection of light pulses from clouds," Appl. Opt. **10**, 2304–2310 (1971).
8. W. G. Blättner, D. G. Collins, and M. B. Wells, "The effects of multiple scattering on backscatter lidar measurements in fog," Proj. Rep. RRA-T7402 (Radiation Research Associates, 1974), available as AD-78180116GI (National Technical Information Service, Springfield, Va.).
9. K. E. Kunkle and J. A. Weinman, "Monte Carlo analysis of multiply scattered lidar returns," J. Atmos. Sci. **33**, 1772–1781 (1976).
10. D. T. Gillespie, "A theorem for physicists in the theory of random variables," Am. J. Phys. **51**, 520–533 (1983).
11. D. T. Gillespie, "Analytic reduction of the monostatic lidar multiple backscattering integral," Rep. NWC TP 6605 (Naval Weapons Center, China Lake, Calif., 1985).
12. As used here, the term "scattering" refers only to elastic encounters between a photon and a cloud particle in which the photon's energy and hence wavelength do not change. An inelastic encounter is considered to be an "absorption," since any shift in a photon's wavelength is presumed to render it invisible to the monochromatic receiver.
13. Letting $P(u)$ denote the probability on the right-hand side of Eq. (4), then the multiplication law of probability theory implies that $P(u + du)$ is equal to $P(u)$ times the probability $(1 - \beta du)$ that nothing will happen to the photon between u and $u + du$. This equality leads immediately to the differential equation $dP/du = -\beta P$, whose solution, subject to the obvious requirement $P(0) = 1$, is $\exp(-\beta u)$.
14. These variables are *algebraically* independent because they satisfy no algebraic equation that can be solved for some one of the variables in terms of the others. However, these variables are not *statistically* independent, since their joint probability density function ($\propto Q_n$) cannot be factored into a product of single-variable functions.
15. We should really distinguish between a random variable and its possible values by using different symbols for each. For example, T might be used to represent the random variable "total photon travel time," whereas t could be the dummy real variable repre-

senting the possible values that T may assume. However, to avoid a proliferation of notation, we shall use the same symbol t for both of these quantitites, hoping that our meaning will always be clear from the context.
16. The rule for transforming delta functions is discussed in D. T. Gillespie, "Addenda to 'A theorem for physicists in the theory of random variables,' " Rep. NWC TP 6462 (Naval Weapons Center, China Lake, Calif., 1983).
17. D. T. Gillespie, "The Monte Carlo method of evaluating integrals," Rep. NWC TP 5714 (Naval Weapons Center, China Lake, Calif., 1975). Available from National Technical Information Center, Springfield, Va.